COMPARISON OF MACROTEXTURE MEASURING DEVICES USED IN VIRGINIA

ManQuan Huang

Thesis submitted to the Faculty of the Virginia Polytechnic Institute and State University in partial fulfillment of the requirements for the degree of

Master of Science
In
Civil Engineering

Gerardo W. Flintsch, Chair
Imad L. Al-Qadi
Amara Loulizi

May 13, 2004
Blacksburg, Virginia

Keywords: Pavement Macrotexture, Texture Measurement, Correlation, Mean Profile Depth (MPD)

COMPARISON OF MACROTEXTURE MEASURING DEVICES USED IN VIRGINIA

MANQUAN HUANG

(ABSTRACT)

This thesis compared macrotexture measurements obtained using the volumetric method (Sand Patch) and three laser-based devices: MGPS system, ICC laser profiler, and Circular Texture Meter (CTMeter). The study used data from three sources: two controlled experiments conducted at the Virginia Smart Road, field data collected on eight newly constructed hot-mix-asphalt (HMA) roadway surfaces, and data collected on airport surfaces at the Wallops flight facility, Virginia.

The data collected at the Virginia Smart Road, a controlled-access two-lane road that includes various HMA and concrete surfaces, was used for the main analysis. The other two sets of data were used for verification and validation of the model developed. The analysis of the data collected at the Virginia Smart Road showed that the CTMeter mean profile depth (MPD) has the highest correlation with the volumetric (Sand Patch) mean texture depth (MTD). Furthermore, texture convexity had a significant effect on the correlation between the measurements obtained with different devices.

Two sets of models for converting the laser-based texture measurements to an estimated MTD (ETD) were developed. One set of equations considered all the data collected at the Virginia Smart Road, and the other excluded the measurements on the Open-Graded Friction Course (OGFC). The developed models were tested using measurements collected at eight roadway sections throughout Virginia and the Wallops flight facility. The model, excluding the OGFC section, was successfully applied to other sites.

ACKNOWLEDGMENTS

I would like to express my sincere gratitude to my advisor, Dr. Gerardo Flintsch, for his guidance, confidence, and patience throughout the process to complete this research, also for his always kind help during the two years when I studied at the Virginia Tech. In addition, great thanks are given to my committee members, Dr. Imad Al-Qadi and Dr. Amara Loulizi, for their knowledge and guidance they contributed to this research.

I would also like to thank the people who helped with testing throughout the research, including Kevin McGhee from VTRC for his help with profiling, and Edgar de Leon and Carlos Rafael Gramajo from VTTI for their help with CTMeter measurements.

Thanks also go to my colleagues at VTTI for their support and friendship throughout the past two years. Thank you, Alan, Billy, Chen, Jun, Kun, Mostafa, Samer K, Samer L, ShihHsien, and the rest of the Roadway Infrastructure Group, thanks for the days we spent together; they will be always treasured for my whole life.

Finally, I would like to express my highest gratitude to my family for their support and love during my whole life. Thanks a lot to my parents for their selfless support and love. Thanks a lot to my dear wife for her always love and for her support and understanding during the days being separated. Thanks a lot to my brother and sisters for their encouragement and guidance.

TABLE OF CONTENTS

LIST OF TABLES

LIST OF FIGURES

CHAPTER 1
INTRODUCTION

1.1. BACKGROUND

Surface texture is a very important feature of the pavement surface, affecting friction, tire wear, exterior vehicle noise emission, interior vehicle noise emission, light reflection, and rolling resistance (Nordic, 1999). Tire-pavement friction is affected by the presence of water on the pavement surface. This water reduces the interaction area, which induces hydroplaning, reduces skid resistance, and adversely affects vehicle control. Thus, pavement texture should supply not only enough tire-pavement interaction, but also quick drainage during precipitation.

A survey of state agencies in the United States, provinces in Canada, and countries in Europe and Asia (Henry et al., 2000) ranked the relative importance of various pavement surface properties as follow (1 is very important and 3 is relatively unimportant):

- Durability (1.2)
- Friction (1.3)
- Splash and spray (1.9)
- Exterior noise (2.3)
- In-vehicle noise (2.4)
- Rolling resistance (2.7)
- Tire wear (2.8)

Similar rankings were obtained for U.S. agencies and non-U.S. agencies. Furthermore, the investigation determined that these pavement properties are mainly affected by pavement surface, vehicle operation conditions, and tire-pavement interaction.

According to the wavelength of surface irregularities, pavement surface texture can be divided into four categories: microtexture, macrotexture, megatexture and roughness (Henry, 2000). Macrotexture plays an important role in maintaining satisfactory

pavement friction level (Dupont et al., 1995). To make pavements safe for riders, transportation agencies need to maintain their pavements with adequate macrotexture.

The technology for direct macrotexture measurement is well developed; today's laser-based macrotexture measuring devices can measure the surface profile at traffic speeds. However, available macrotexture measuring devices do not necessarily measure the same surface properties and thus produce different measurements. Hence, it is important to determine the most appropriate method for measuring macrotexture. In addition, it is necessary to investigate whether it is possible to harmonize the various macrotexture measurements obtained with different devices to a standard macrotexture measurement.

This thesis focused on correlating the macrotexture measurements obtained using the volumetric method (Sand Patch) and three laser-based devices: MGPS system, ICC laser profiler, and Circular Texture Meter (CTMeter) at the Virginia Smart Road. Furthermore, two sets of models were developed to convert the laser-based macrotexture measurements to an Estimated Mean Texture Depth (ETD). These models were tested using three additional data sets and the best-predicting models were recommended for implementation.

1.2. PROBLEM STATEMENT

Different devices with macrotexture measurement capability are available. However, these devices may not measure the same surface properties; and thus they could produce different macrotexture measurements. The differences could be operational or due to data analysis methodology used to compute the surface texture statistics. Hence, a need exist to select a reference measurement technique and correlate measurements by different devices to the reference one.

1.3. OBJECTIVES

To address the aforementioned problem, the main objective of this study is to correlate macrotexture measurements using three different devices to a ground truth volumetric measurement (Sand Patch). Three laser-based devices –MGPS system, ICC laser

profiler, and CTMeter– were selected. In order to achieve this objective, measurements repeatability, and surface texture convexity effect, and type of surface mix effect must be investigated.

1.4. RESEARCH APPROACH

Tests conducted on seven surfaces at the Virginia Smart Road included macrotexture measurements obtained with the Sand Patch, MGPS System, ICC profiler, and CTMeter. The data collected were used to determine the repeatability of the laser-based devices; the relationship among the various macrotexture measurements; and the effect of texture convexity or type of surface mix; as well as to develop models to convert the laser-based measurements to ETD.

Three additional data sets were used to validate the models:

1. Another data set collected at the Virginia Smart Road, using the ICC profiler and the CTMeter.
2. Data collected on eight typical highway pavement surfaces throughout Virginia, and
3. Macrotexture measurements collected on airport surfaces at the Wallops flight facility.

1.5. THESIS SCOPE

This thesis is divided into five chapters. Chapter Two provides an introduction to pavement surface texture, commonly used macrotexture measuring methods, and applications of macrotexture measurements, and presents a review of relevant macrotexture measurement studies. Chapter Three presents a detailed analysis of the main data set. Chapter Four validates the models developed in Chapter Three using the other three sets of data. Findings and conclusions of the research program are presented in Chapter Five.

CHAPTER 2
LITERATURE REVIEW

This chapter provides an introduction to macrotexture measurements, by discussing the following issues: pavement texture classification, techniques for macrotexture measurement, related macrotexture comparison studies, and applications of macrotexture measurements.

2.1. PAVEMENT TEXTURE CLASSIFICATION

According to the wavelength of surface irregularities, pavement surface texture can be divided into four categories (Henry et al., 2000):

- Microtexture: Those surface irregularities with texture wavelength between 1μm and 0.5mm are defined as microtexture. The typical peak-peak amplitudes of microtexture are between 0.1μm and 0.2mm (ISO 13473-1 & ISO/DIS 13473-2). Microtexture is necessary at all speeds to maintain a satisfactory tire-pavement friction. Microtexture mainly depends on the asperities or microrugosity of the pavement surface, particularly the aggregate, in contact with the tire rubber. The microrugosity is an inherent characteristic of the aggregate, and it is affected by polishing under the action of traffic. According to the literature, skid resistance reductions due to pavement wear vary considerably (Dupont et al., 1995). Microtexture has a negative effect on tire wear (Nordic, 1999).
- Macrotexture: Macrotexture is defined as those irregularities with texture wavelength between 0.5mm and 50mm. Typical peak-to-peak amplitudes of macrotexture are between 0.2mm and 10mm (ISO 13473-1 & ISO/DIS 13473-2). Macrotexture is necessary for providing quick water drainage, which is required to maintain an appropriate pavement friction, especially at medium and high speeds. Macrotexture mainly depends on aggregate gradation, shape and angularity, and is also affected by material engineering, design, and construction. Vehicle tires can compensate for a poor macrotexture to maintain good pavement friction, but not for a poor microtexture (Dupont et al., 1995). Besides affecting tire-pavement friction, macrotexture is found to have a significant effect on

rolling resistance, fuel consumption, and exterior and interior noise (Nordic, 1999).

- Megatexture: Megatexture is defined as those irregularities with texture wavelength between 50mm and 500mm. Typical peak-to-peak amplitudes of megatexture are between 1mm and 50mm (ISO 13473-1 & ISO/DIS 13473-2). Megatexture affects rolling resistance, riding comfort, vehicle wear, and noise (Dupont et al., 1995).
- Roughness: Smoothness, roughness, or unevenness is comprised of those irregularities with texture wavelength between 0.5m and 50m. According to Permanent International Association of Road Congresses (PIARC), roughness is divided into three categories: unevenness of small wavelength, unevenness of medium wavelength, and unevenness of large wavelength (Figure 2-1). Roughness is found to have the most effects on ride quality, and vehicle control (Dupont et al., 1995).

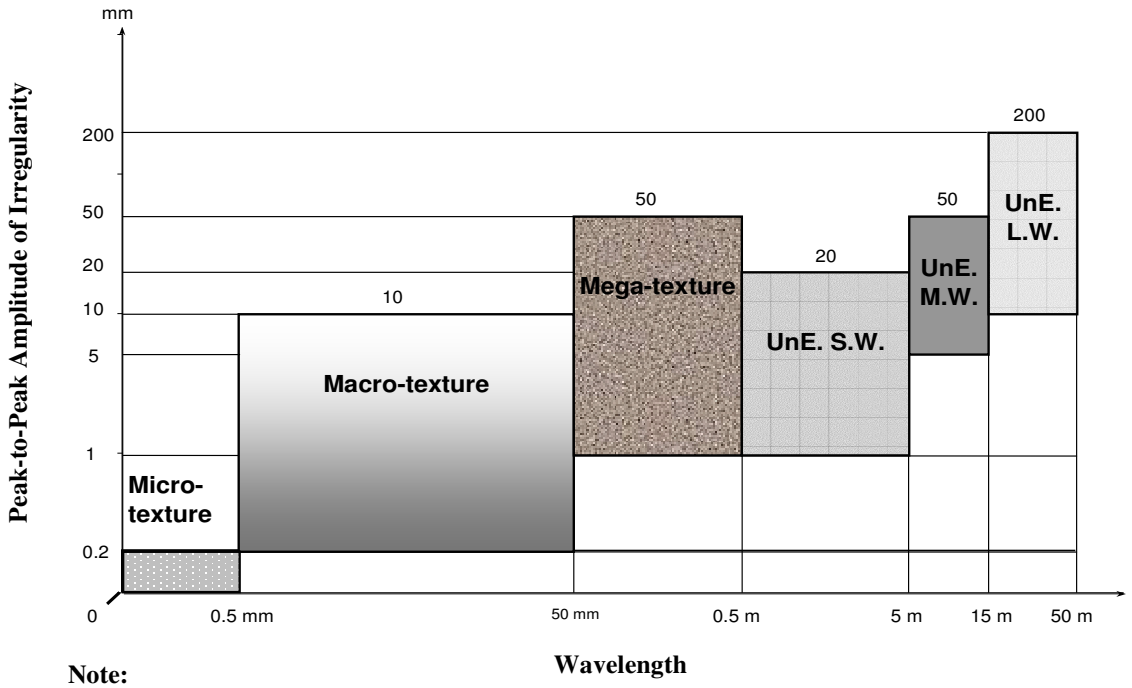

Note:

UnE. S.W. = Unevenness (Roughness) of small wavelength
UnE. M.W. = Unevenness (Roughness) of medium wavelength
UnE. L.W. = Unevenness (Roughness) of large wavelength

Figure 2-1 Surface Texture Classifications

2.2. MACROTEXTURE MEASURING TECHNIQUES

The technology for direct macrotexture measurement is well developed. Because of increasing recognition of the important role of pavement macrotexture in providing adequate skid resistance, macrotexture measurement is becoming widely used in the United States. Traditionally, macrotexture has been measured using a manual volumetric technique. However, developments of laser technology and computational power and speed have allowed researchers to develop equipments to measure macrotexture at traffic speeds (Abe et al., 2000).

Currently used methods for macrotexture measurement can be classified into three types: volumetric technique, outflow method, and laser-based methods. Laser-based methods include dynamic methods, such as laser profilers that can operate at traffic speeds, and "static" methods, such as the Circular Texture Meter (CTMeter).

2.2.1. Volumetric Method

In the volumetric technique (ASTM E965 – 96), the average depth of pavement surface macrotexture is determined by careful application of a known volume of material on the surface and subsequent measurement of the total area covered. Dividing the volume by the area covered provides the mean texture depth (MTD). Variations of this method are referred to as the sand patch, sand track, or grease patch methods. Originally sand was used as the spreading material. However, the current standard uses glass spheres because glass spheres spread more uniformly than sand, which has an irregular shape, and very low yields are usually obtained when bags of sand are sieved, whereas glass spheres that meet the size specification are commercially available and the need to sieve the material is avoided (Abe et al., 2000). The Virginia DOT still uses sand as the spreading material (Figure 2-2).

Figure 2-2 Sand Patch Test on the Virginia Smart Road

The procedure for the volumetric method is the following (ASTM E965-96):

- Test Area: Inspect the pavement surface to be measured and select a dry, homogeneous area that contains no unique localized features such as cracks and joints. Thoroughly clean the surface using the stiff wire brush first and subsequently the soft bristle brush to remove any residue, debris, or loosely bonded aggregate particles from the surface. Position the portable wind screen around the surface test area.
- Material Sample: Fill the cylinder of known volume with dry material and gently tap the base of the cylinder several times on a rigid surface. Add more material to fill the cylinder to the top, and level with a straightedge. If a laboratory balance is available, determine the mass of the material in the cylinder and use this mass of material sample for each measurement.
- Test Measurement: Pour the material onto the cleaned surface within the area protected by the wind screen. Carefully spread the material into a circular patch with the disk tool, rubber-covered side down filling the surface voids flush with the aggregate particle tip. Measure and record the diameter of the circular area covered by the material at a minimum of four equally spaced locations around the sample circumference. Compute and record the average diameter.

- Calculations: Compute the average pavement macrotexture depth (MTD) using the following equation:

$$MTD = \frac{4V}{\pi D^2} \quad (2.1)$$

where:
MTD = Mean Texture Depth of pavement macrotexture, mm (in.),
V = sample volume, mm ^{3}. (in ^{3}), and
D = average diameter of the area covered by the material, mm (in.).

- Number of Test Measurement: ASTM recommends at least four, randomly-spaced MTD measurements on a given test pavement surface type. The arithmetic average of the individual macrotexture depth values shall be considered to be the average macrotexture depth of the tested pavement surface.

2.2.2. Outflow Method

The outflow meter (ASTM STP 583) is a transparent vertical cylinder that rests on a rubber annulus placed on the pavement. This device measures how long it takes a known quantity of water, under gravitational pull, to escape through voids in the pavement texture of the structure being tested. To take a measurement, a valve at the bottom of the cylinder is closed and the cylinder is filled with water. The valve is then opened, and the time in seconds that it takes the level to pass two specific marked levels is measured and recorded as the outflow time (OFT). OFT is measured either by a stopwatch or by an electronic timer (Abe et al., 2000). Since it is the texture that determines the rate of flow of the water, inverse seconds is an indirect measure of texture. On a perfectly smooth plate the time is infinite (Wambold et al., 1995). A faster escape time indicates that a thinner film of water may exist between the tire and the pavement. Thus, more microtexture will be exposed in the tire-surface interface, reducing the potential for hydroplaning under wet condition (ASTM, 2003).

2.2.3. Laser-Based Methods

Several systems that measure macrotexture at traffic speeds are available. These systems measure the pavement profile and then use this profile to compute various surface macrotexture parameters, such as Mean Profile Depth (MPD) and the overall

Root Mean Square (RMS) of the profile height (Abe et al., 2000). Compared to the aforementioned methods, laser-based methods have the following advantages:

- Operator independence;
- Direct reading and automatic macrotexture parameters output;
- Capability of measurement at traffic speeds (dynamic systems only).

The most used macrotexture parameters are presented following. The main characteristics of the three laser-based systems compared in this study (MGPS system, ICC profiler, and CTMeter) are also presented.

MPD Calculation

The following is the process to calculate the MPD (ASTM E1845):

- The measured profile is divided into segments having a length of 100mm (4 in.).
- The slope of each segment is suppressed by subtracting a linear regression of the segment. This provides a zero mean profile, i.e., the area above the reference height is equal to the area below it.
- The segment is then divided in half and the height of the highest peak in each half segment is determined (Figure 2-3).
- The average of these two peak heights is the mean segment depth.
- The average value of the mean segment depths for all segments making up the measured profile is reported as the MPD.

If the MPD is used to estimate the Sand Patch MTD, ASTM E1960 recommends the following equations:

$$ETD = 0.79\ MPD + 0.23 \qquad (2.2)$$

where,
ETD = Estimated Mean Texture Depth, and
MPD = Mean Profile Depth

ISO 13473 and ASTM E1845 recommend the same equation but with the coefficients rounded to 0.8 and 0.2, respectively (Abe et al., 2000).

$$MPD = \frac{\text{Peak level (1st)} + \text{Peak level (2nd)}}{2} - \text{Average level}$$

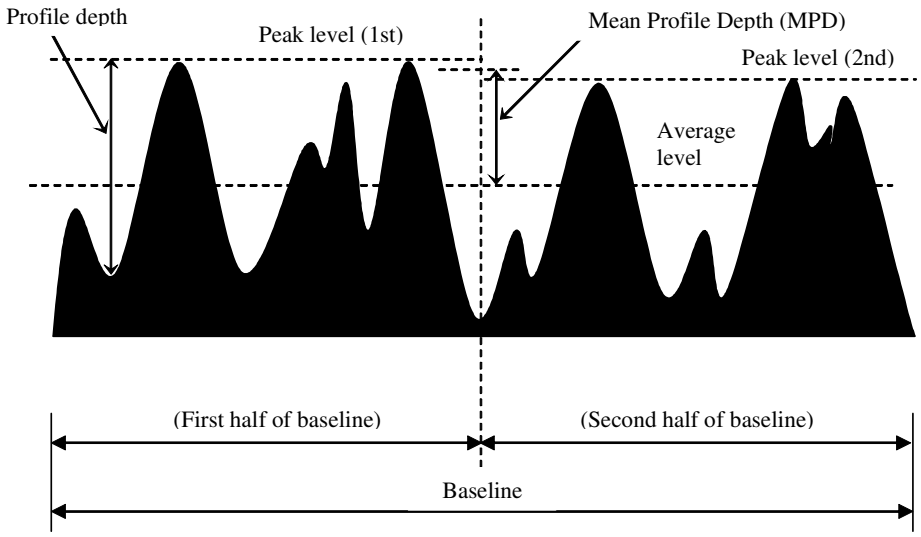

Figure 2-3 Mean profile Depth (MPD) Computation

RMS Calculation

The root mean square value of the profile has also been proposed as a measurement of pavement macrotexture. If there are n measurements (a_1, a_2… a_n) in one baseline profile, the RMS is calculated using the following equation:

$$RMS = \sqrt{\frac{(a_1 - a_{avg})^2 + (a_2 - a_{avg})^2 + ... + (a_n - a_{avg})^2}{n}} \qquad (2.3)$$

where,
a_1… a_n = the macrotexture measurement within one baseline profile,
a_{avg} = the average of the macrotexture measurements within one baseline profile, and
n = the number of macrotexture measurements taken within one baseline profile.

MGPS System

The MGPS system is the commercial outgrowth of the Federal Highway Administration's (FHWA) ROad Surface ANalyzer (ROSAN) project conducted by the Turner-Fairbank Highway Research Center (McGhee et al., 2003). The MGPS system uses a short-range laser range finder, an accelerometer, and a distance measuring transducer to measure and compute the pavement profile. The system can measure

macrotexture, faulting, grooving, rutting, slope, and pavement profile at speeds of up to 120 km/hour (Sixbey et al., 1998). The MGPS system uses a high frequency (64 MHz) laser sensor with a small imprint, which allows it to measure the profile with definition down to 0.25mm if the tests are conducted at slow speeds. The system then uses the profile to compute the standard MPD specified in ASTM E1845 (McGhee et al., 2003). The system also includes software to compute an ETD.

ICC Laser Profiler

The laser profiler manufactured by International Cybernetics Corporation (ICC), which is mounted on the Virginia Transportation Research Council's (VTRC) inertial profiling vehicle (Figure 2-4) is similar to the MGPS system, but uses relatively slower sensors, which makes it comparatively less accurate. However, early findings have shown it is appropriate for most hot-mix asphalt (HMA) surfaces (McGhee et al., 2003). The ICC laser profiler computes an MPD value; however, the calculation is not conducted in accordance with ASTM E1845. It uses a RMS-based proprietary algorithm to compute the MPD.

Figure 2-4 VDOT Laser Profiler on Route 460 in Tazewell, Virginia

Circular Texture Meter (CTM or CTMeter)

The Circular texture meter (CTMeter) uses a laser to measure the profile of a circle 284 mm (11.2in.) in diameter or 892 mm (35in.) in circumference. It can be used both in the laboratory and the field. The profile is divided into eight segments of 111.5 mm (4.4 in.) for analysis, as shown in Figure 2-5.

The mean profile depth (MPD) of each segment or arc of the circle is computed according to the standard practices of ASTM and ISO. The CTMeter is controlled with a notebook computer, which also performs the calculations and stores the MPD of each segment. The average for all eight segments, the average for the two Arcs that are perpendicular to the travel direction, and the average for the two segments in the direction of travel are computed (Abe et al., 2000).

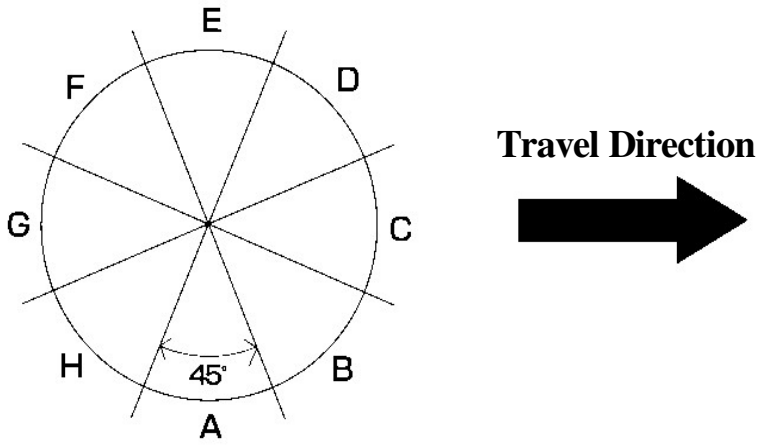

Figure 2-5 Segments of the Circular Texture Meter

The CTMeter software reports the MPD and RMS values of the macrotexture profiles (ASTM E 2157). The following equations have been used to convert the MPD computed by the CTMeter to MTD (ASTM E 2157):

$$MTD = 0.947\ MPD_{CTM} + 0.069 \qquad (2.4)$$

where,
MTD and MPD_{CTM} are expressed in millimeters,

or:

$$MTD = 0.947\ MPD_{CTM} + 0.0027 \qquad (2.5)$$

where,
MTD and MPD_{CTM} are expressed in inches.

The standard test procedure for measuring pavement macrotexture properties using the CTMeter is the following (ASTM E 2157):

- Place the CTMeter on the test surface which should be free of any contamination (Figure 2-6). Segments C and G should be perpendicular to the direction of travel.
- Select the option to compute MPD, RMS, or both, and initiate the measurement from the notebook computer.
- Record the test results or store the data for future analysis.

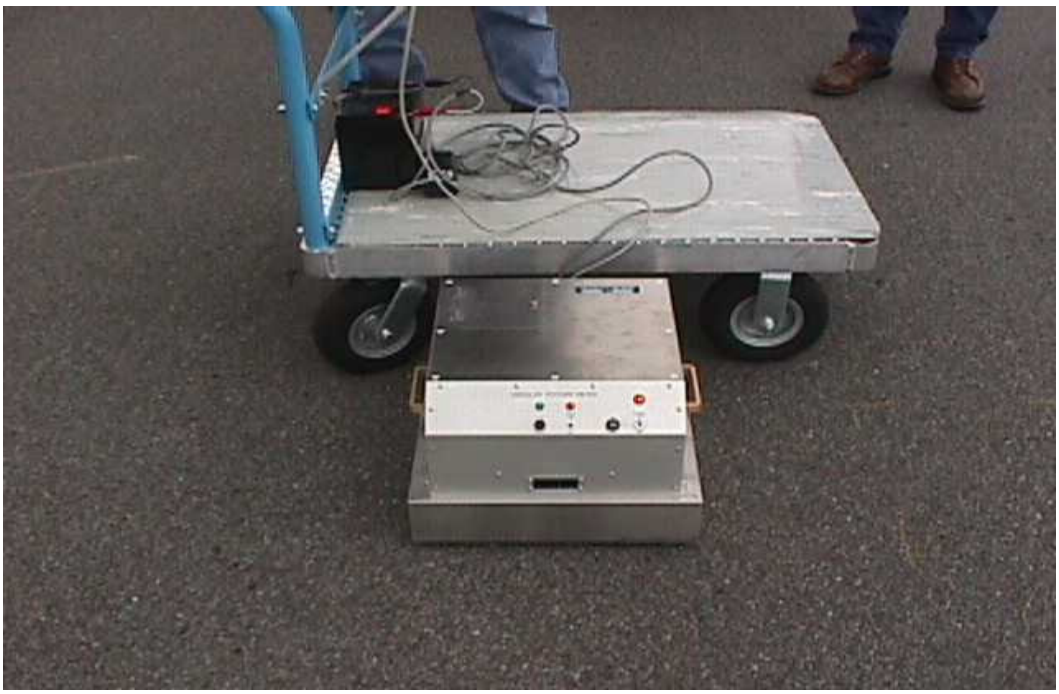

Figure 2-6 Macrotexture Measurement Using CTMeter on the Virginia Smart Road

2.2.4. Texture Convexity

Comparison of the MPD and the RMS for a surface provides information on the nature of the texture convexity, that is, whether the texture orientation or convexity is positive, negative, or neutral. Examples of pavement surfaces with positive and negative texture are presented in Figure 2-7. A positive texture means macrotexture is produced by asperities projecting above the surface. A negative texture is produced by depressions in the surface (ASTM E 2157). The following method can be used to determine whether a texture is positive, negative or neutral (McGhee et al., 2003):

- If, MPD>RMS, and [(MPD-RMS)/RMS]>5%, the texture can be defined as positive texture;
- If, RMS>MPD, and [(RMS-MPD)/MPD]>5%, the texture can be defined as negative texture;
- Otherwise, the texture can be defined as neutral texture.

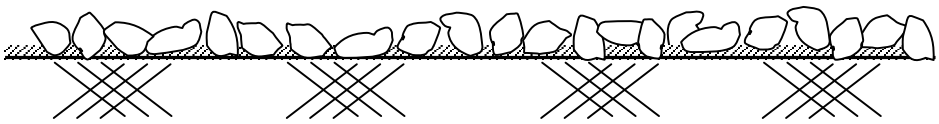

(a) Chip Seal (Positive Texture)

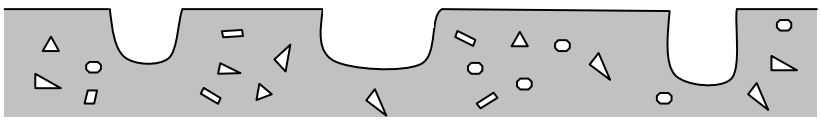

(b) Grooved Concrete (Negative Texture)

Figure 2-7 Examples of Positive and Negative Texture

2.2.5. Comparison of Different Macrotexture Measuring Methods

A summary comparison of all the different macrotexture measuring methods mentioned is presented in Table 2-1 (McGhee et al., 2003).

Table 2-1 Macrotexture Measuring Methods Comparison

Name	Type of System	Background	Frequency of Meausurement	Measures
Volumetric Method (Sand Patch)	Static	Traditional	Semi-Continuous	MTD
Outflow Meter	Static	Traditional	Continous	OFT
ICC Laser Profiler	Dynamic	Developed by ICC	Discrete	MPD*
MGPS System	Dynamic	Developed by FHWA (Commerial outcome of ROSAN project)	Discrete	MPD
CTMeter	Static	Developed by Nippon Sangyo Co. of Japan	Discrete	MPD & RMS

***Note: The ICC MPD is estimated using a proprietary algorithm, not consistent to ASTM E 1845.**

2.3. MACROTEXTURE MEASUREMENT COMPARISON STUDIES

There have been several studies conducted to investigate the relationship between macrotexture measurements obtained with different types of devices. Two of those studies are summarized in the following sections. In these studies, the following two properties were proposed to evaluate the macrotexture measuring devices (Andresen, et al., 2003):

- Repeatability: how much the reported texture values of a device differ for repeated measurements over the same set of surfaces, and
- Reproducibility: how much the reported texture values of a fleet of the same generic type of devices differ over a range of texture values

2.3.1. International PIARC Experiment to Compare and Harmonize Texture and Skid Resistance Measurements

This experiment (Wambold, et al., 1995) compared friction and texture measurements obtained with different equipments and technologies and defined an international scale of friction values called IFI (International Friction Index). The study was sponsored by the Permanent International Association of Road Congresses (PIARC). One important contribution is that this experiment formally recognized the need to consider surface texture in order to relate friction data obtained with different measurement methods.

Models incorporating pavement texture characteristics were used to analyze the pavement friction data.

The overall objective of the experiment was to harmonize the many different pavement friction measurement methods used in different countries around the world. The specific objectives are listed following:

- Develop and evaluate relationships between friction and texture measurements obtained with various measurement devices under varying physical test conditions including texture, speed, slip angle, test tire, climate, and materials.
- Quantify relationships between standard measures of friction and texture obtained with the various devices under specific conditions to facilitate interchange and harmonization of technical information.
- Quantify the repeatability and measurement errors associated with the various devices.

Friction and texture were measured simultaneously on a large number of pavements exhibiting a wide range of friction and texture. The experiment was conducted in September and October of 1992, and included 54 sites: 28 in Belgium (2 at an airfield, 4 at a race track and 22 on public roads) and 26 in Spain (8 at airfields and 18 on public roads). All measurements were completed in as short a period of time as possible in order to avoid large temperature differences or other changes which may occur as the day progresses. There were 51 different measurements made with equipment from 16 countries. All texture measurements were made on dry surfaces before any water was applied to the roadway.

Macrotexture Measuring Devices Considered

Fourteen devices were used to measure macrotexture in the PIARC experiment, which covered the commonly used three types of texture devices: texture profilometers, volumetric method, and outflow meter. The outputs from these devices included MTD (Mean Texture Depth), MPD (Mean Profile Depth), RMS (Root Mean Square of Profile Depth), and OFT (Outflow Time).

Macrotexture Analysis

In this experiment, the texture data were analyzed to investigate the following five statistics:

- Correlations between the volumetric MTD measurements and other texture measures,
- Correlation between texture measures for all measures and devices,
- Inter-correlations in texture,
- Optimum texture wavelengths for estimation of MTD, and
- Correlation between Outflow meters and other texture measuring devices.

A brief overview of the first two analyses is presented in the following sections.

Correlations between MTD and Other Texture Measures

The first step to calibrate the various texture measuring devices was to investigate the relationship between the MTD (by the volumetric patch) and the measurements obtained with the other texture measuring devices. If the measurements from the other devices can be related to the volumetric patch measurements by a linear equation, then this equation can be used for standardization or calibration of the devices. This also provides an excellent means by which other devices which were not included in the experiment could be calibrated in the future. The following conclusions were drawn from this analysis:

- It is possible to accurately predicted MTD from profile measurements using linear models: very high correlations were obtained between the measurements obtained with the volumetric patch and other texture measuring devices.
- RMS-based measures are not comparable to the volumetric method results, unless some transformation equation is applied.
- Most of the mean predicted texture depths are rather close to the measured ones, though the maximum and minimum values experienced more variation.
- It is necessary to include a correction for slope of the profile curve to minimize the influence of megatexture and unevenness on the calculation of an alternative measure to MTD. This correction has been included in the ASTM procedure.

Correlation between All Texture Measurement Methods and Devices

In this step, every measure (Y) was correlated to all the others (X) using linear regression: Y = A*X + B and the following conclusions were drawn:

- All the non-contact profiling devices are able to deliver at least one macrotexture measure that correlate to at least one of the other devices with a coefficient of correlation R > 0.94.
- The correlation coefficient between the measurements reported by the profiling devices and the MTD determined by the volumetric patch test ranged from .402 to .966. In general, measurements based on the MPD concept are better than those based on the profile RMS-value, though some RMS-based measurements still correlate better with MTD than certain MPD-based measurements.
- The volumetric patch test is significantly biased by the finite size of the granular material used: texture depths lower than .25mm can not be measured and texture up to 1 mm may be influenced significantly.

2.3.2. Norwegian Comparison of Pavement Texture Measurement Systems

The Norwegian Roads Administration conducted a texture workshop in April, 2002 to compare a fleet of instrumented vans acquired to survey the national road network. The experiment was conducted at Oslo Airport, Gardermoen (Andresen, et al., 2003).

The owner and operator of Norwegian airports constructed the Ottar K. Kollerud Test Track located at the new Oslo airport as a field laboratory site for runway surface tests in 1997. The test track, also known as the OKK test track, includes ten different asphalt pavement sections, which are 100m long and 10m wide. Eight of these sections are used to harmonize devices measuring surface characteristics. The specific objectives of the workshop were the following:

- Determine the repeatability of the devices engaged.
- Determine the reproducibility of the devices engaged.
- Determine the performance of a sub routine of the laser signal processing software to remove the effects of surface grooves on the reported texture values.

- Determine a relationship of the non-contact texture measurements with a volumetric contact measuring method.
- Determine a harmonization relationship among the non-contact texture measuring systems.
- Investigate potential relationships between the texture measurements and pavement friction.

The test sections are equally divided across their width into 5 segments. The seven laser instrumented vans ran three distance calibration runs in lane A and then 6 repeated test runs on three of the five segments (A, B & D). The distance measured in each lane was 1060m. The target measuring speed was 50 km/h. After the laser instrumented vans completed their measurements, volumetric texture measurements were taken on lanes B and D in accordance with ASTM International standard E-965. The following conclusions were drawn from the workshop:

- The overall or fleet average range of variability for an individual vehicle including all test track surfaces was 3.8%. The average repeatability coefficient of variation of the non-contact texture measurement systems was 1.4% for non-grooved surfaces, and 1.9% for grooved surfaces.
- The average reproducibility coefficient of variation for all devices and segments was 4.0%.
- When disregarding the open, coarse surface types, there seemed to be no effect of surface grooves on the average MPD values for each measured lane.
- MTD values can be predicted from MPD measurements using a transformation equation.
- High correlation coefficient and rather low standard error were obtained when harmonizing all the non-contact texture devices using linear regression.

2.4. APPLICATIONS OF MACROTEXTURE MEASUREMENT

One of the main applications of macrotexture measurement is to predict pavement friction. The International Friction Index (IFI), which was developed in the aforementioned PIARC international experiment (Wambold et al., 1995), uses

macrotexture measurements to predict the change of friction with speed (ASTM E 1960). Besides this, macrotexture measurement can also be used for detecting and quantifying HMA segregation or non-uniformity (Flintsch et al., 2003-b). Other applications include tire/road noise determination. The applications for IFI calculation and surface segregation detection are introduced following.

2.4.1. International Friction Index (IFI) Calculation

The IFI allows for harmonizing friction measurements with different equipment to a common calibrated index. The IFI consists of two parameters: the calibrated wet friction at 60 km/h (F60) and the speed constant of wet pavement friction (S_p),and it is reported as IFI (F60, S_p).

The speed constant (S_p in km/h) is computed using the following equation (ASTM E 1960):

$$S_p = a + b \times TX \tag{2.6}$$

where,
TX = Macrotexture measured using a specific method, and
a and b = Constants that depend upon the method used to determine the macrotexture as given in Table 2-2.

Table 2-2 Values of a and b for Estimating the Speed Constant (Sp)

TX	a	b
MPD per Practice E 1845	14.2	89.7
MTD per Test Method E 965	-11.6	113.6

To calculate F60, first the friction FRS measured at the slip speed S needs to be adjusted to the friction at 60km/h, FR60, using the following transformation equation:

$$FR60 = FRS \times EXP[(S - 60)/S_p] \tag{2.7}$$

where:
FR60 = Adjusted value of friction from a slip speed of S to 60 km/h for the equipment,
FRS = Friction measured by the equipment at slip speed S, and
S = Slip speed of the equipment.

The calibrated Friction Number F60 is then computed using the following harmonization equation:

$$F60 = A + B \times FR60 + C \times TX \qquad (2.8)$$

where,
A, B, and C = Calibration constants for a particular friction measuring device; if the device uses a blank tire, C is 0.

The calibration constants are given in the Appendix X1 of ASTM E 1960 for devices calibrated during the PIARC experiment. For other devices, a calibration must be performed to establish the A, B, and C for that particular device.

2.4.2. Macrotexture Measurement for Assuring Pavement Surface Uniformity

Segregation has long been one of the major problems in HMA production and placement. A segregated mix does not conform to the original Job Mix Formula (JMF) in gradation and/or asphalt content, creating a difference in the expected density and air void content of the mix (Flintsch et al., 2003-b). Research has shown that when this happens, there is a loss of pavement service life because of diminished stiffness, tensile strength, and fatigue life, resulting in accelerated pavement distresses such as raveling, longitudinal cracking, fatigue cracking, and rutting (Cross et al., 1993; Khedaywi et al., 1996).

Traditionally, segregation problems of HMA pavements are first identified through a subjective visual assessment. This too frequently results in disputes between contractors and highway agencies. Many studies have attempted to develop reliable and independent methods to define, detect, and quantify segregation, but few have offered a feasible alternative to the initial visual inspection (Flintsch et al., 2003-b). A recent study conducted in Virginia (McGhee et al., 2003), evaluated three approaches for detecting and quantifying HMA segregation using pavement surface macrotexture measurement. These included applying the methods proposed in NCHRP report 441 (Stroup-Gardiner et al., 2000), which based on predicting the expected “non-segregated” macrotexture; using acceptance bands for texture similar to those used for HMA density; and considering the standard deviation of the macrotexture measurements as a surrogate for construction

uniformity. This investigation concluded that macrotexture measurement may be a useful tool to detect and quantify segregation for quality-assurance purposes.

The study also established the following equations to predict the estimated MTD using measurements obtained with the ICC profiler and CTMeter:

$$ETD = 0.78\ ICCTEX - 0.38 \quad (2.9)$$

$$ETD = 0.98\ MPD_{CTM} + 0.04 \quad (2.10)$$

where,
ETD = Estimated Mean Texture Depth;
ICCTEX = Estimate of macrotexture as computed by the ICC proprietary algorithm;
MPD_{CTM} = Mean Profile Depth computed by the Circular Texture Meter

However, further testing was recommended to test the applicability of these equations to other mixes.

Flintsch et al. (2003) proposed a uniformity specification for HMA construction. This approach is based on the assumption that variability (standard deviation) of texture fluctuates proportionally (and consistently) with the Aggregate Nominal Maximum Size (ANMS). If the variability of texture increases, the material/placement process should have been at least temporarily under less control (less uniform), and thus the pavement should have at least some level of segregation. Reasonable targets for standard deviation of texture were established for different aggregate sizes.

CHAPTER 3
DATA ANALYSIS AT THE VIRGINIA SMART ROAD

3.1. INTRODUCTION

The Virginia Smart Road contains a 3.2km fully instrumented pavement test facility. Located in Montgomery County, Virginia, once completed, the Virginia Smart Road will be a connector road between US 460 and Interstate 81. At present, the Virginia Smart Road is a two-lane controlled-access road, composed of 14 pavement sections. Measurements on seven of these sections (Table 3-1), were conducted for this investigation. Only one lane (East Bound, EB) was measured for most sections. However, both lanes were measured for Sections J and Section K (Open-Graded Friction Course, OGFC).

Table 3-1 Test Surfaces at the Virginia Smart Road

Section ID	Width (m)	Length (m)	Surface Description (VDOT Designation)
Loop	4.9	173.7	Stone Matrix Asphalt (SMA 19)
A	7.3	96.6	Dense-graded HMA (SM 12.5D)
G	7.3	83.5	Dense-graded HMA (SM 9.5D)
J	7.3	85.3	Dense-graded HMA (SM 9.5D)
K	7.3	79.9	Open-Graded Friction Course (OGFC 12.5)
L	7.3	96.6	Stone Mastic Asphalt (SMA 12.5)
Concrete	7.3	76.2	Continuously Reinforced Portland Cement Concrete (Transversely Tined)

Two sets of data were collected at the Virginia Smart Road. The measurements taken on April 9, 2002, using the Sand Patch (SP), Circular Texture Meter (CTMeter), ICC Laser Profiler, and MGPS on sections Loop, A, G, J, K, L, and Concrete, were used for modeling the relationships among the measurements of the various devices. Additional tests conducted on August 17, 2001, using only the ICC profiler and CTMeter, were used to test the developed models.

Six measurements were taken on each section, three on the Left Wheel Path (LWP) and three on the Between Wheel Path (BWP), separated 23.6m (77.5ft), 46.5m (152.5ft) and 69.3m (227.5ft) from the western end of the section (Figure 3-1). The Sand Patch

and CTMeter measurements were conducted on the same locations. The ICC profiler and MGPS system measured the entire LWP and BWP of the sections. However, measurements on 1.5m (5ft) centered on the locations of the static tests were extracted for comparisons with the Sand Patch and CTMeter measurements.

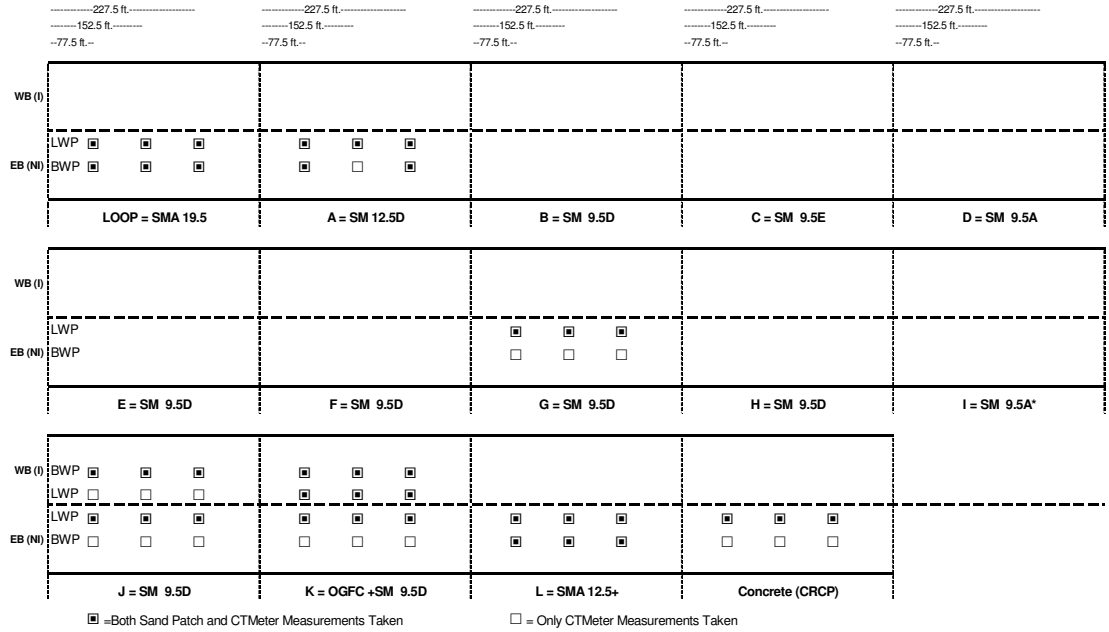

Figure 3-1 Locations of Measurements on April 9, 2002 at the Virginia Smart Road

The macrotexture measurements obtained with these 4 devices for each section were compared in Figure 3-2. The ICC macrotexture values are in general larger than others: on average 89% larger than the SP MTD, 96% larger than the CTMeter MPD and 65% larger than the MGPS MPD. The large difference between the ICC measurements and the other measurements may be due to the specific method used by the ICC profiler to calculate the MPD. While the ICC MPD is estimated using a proprietary algorithm, not consistent with ASTM E 1845, the other devices calculate the MPD using the ASTM method. Hence, the ICC macrotexture measurements are referred as ICC Texture (ICCTEX), rather than MPD, in this thesis.

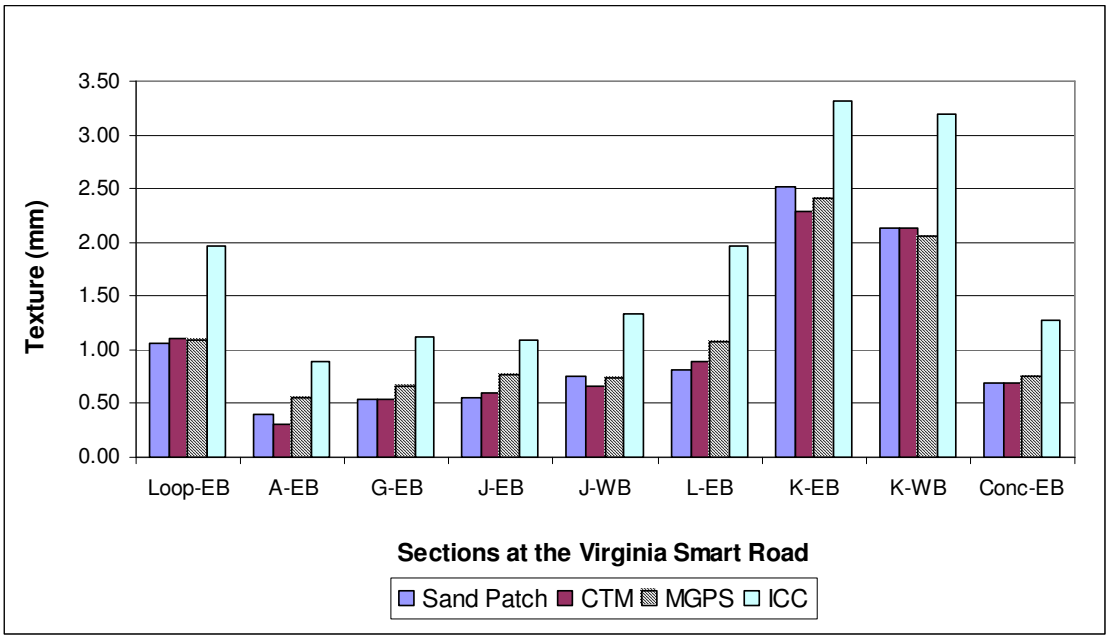

Figure 3-2 Comparisons of Laser-Based Macrotexture Measurements

3.2. REPEATABILITY OF LASER-BASED DEVICES

It is important for a measuring device to have high repeatability. A higher repeatability means a more stable and reliable measurement. The two statistics commonly used to evaluate the repeatability of measures from an instrument, standard deviation (SD) and coefficient of variation (CV), were used in this study (detailed data presented in Appendix A). Figure 3-3 shows the Tukey plot of the average macrotexture measurement of each device at the Virginia Smart Road with 95% confidence limits. The Tukey plot indicates that the CTMeter measurements have less variation than the other two devices.

3.2.1. Standard Deviation (SD)

Figure 3-4 compares the standard deviation of the measurements obtained with the three devices. The CTMeter (with an average SD of 0.036mm) appears to be more repeatable than the MGPS system (with an average SD of 0.073mm) and the ICC profiler (with an average SD of 0.168mm).

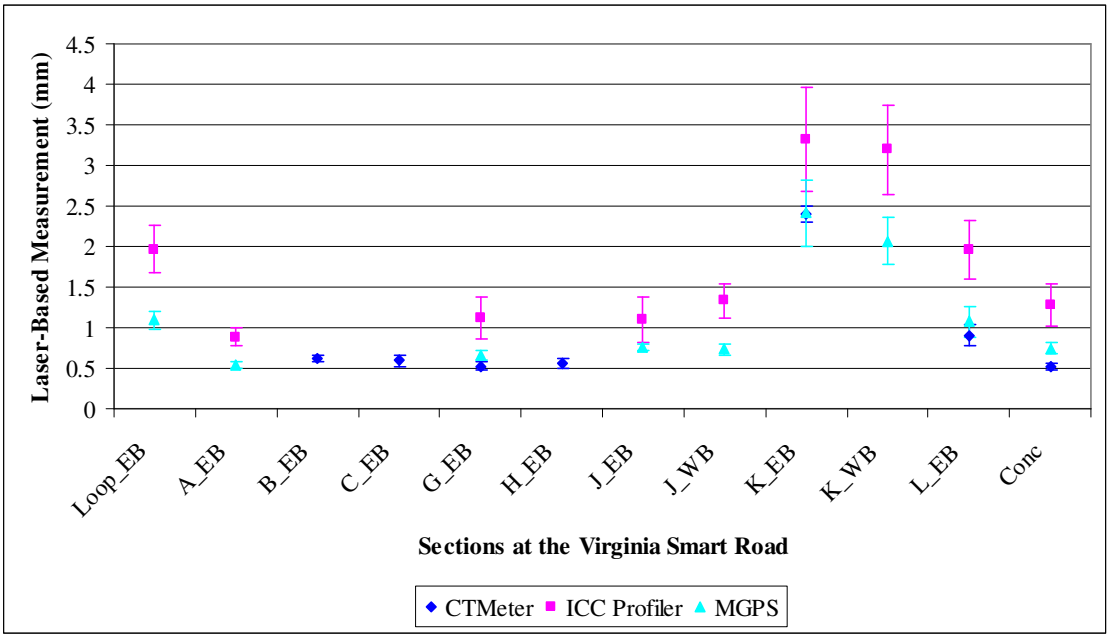

Figure 3-3 Tukey Plot of Laser-Based Macrotexture Measurements

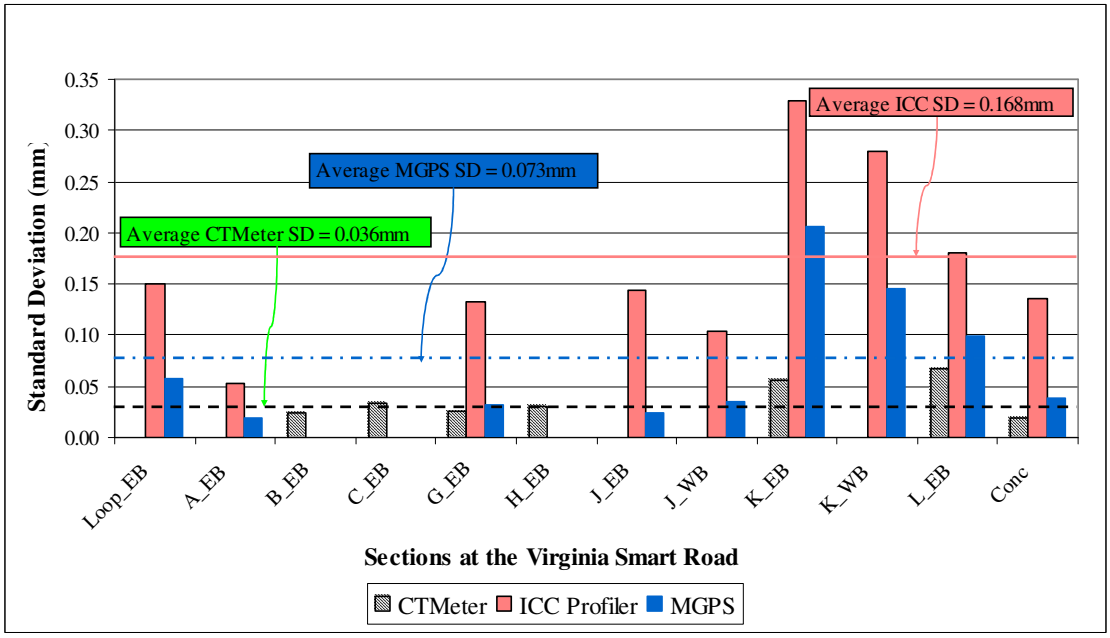

Figure 3-4 Standard Deviation of Laser-Based Macrotexture Measurements

3.2.2. Coefficient of Variation (CV)

The Coefficient of Variation (CV) is another statistic that is commonly used to evaluate the repeatability of measuring devices. The CV is calculated using the following equation:

$$CV(\%) = \frac{\text{Standard Deviation}}{\text{Average}} \times 100\% \qquad (3.1)$$

The CV is a better index than the SD for evaluating the variation of a device because: (1) the CV has no dimensions, which means the units chosen for the measurements will not affect the value of the CV; and (2) the SD of the measurements is usually proportional to the values of the measurements, which means that those measurements with higher values usually have higher standard deviation (Wambold, et al., 1995).

The comparison of the coefficients of variation of the measurements obtained with the three devices, presented in Figure 3-5, is consistent with the previous finding: the CTMeter (with an average CV of 4.7%) appears to be more repeatable than the MGPS system (with an average CV of 5.6%) and the ICC profiler (with an average CV of 9.4%).

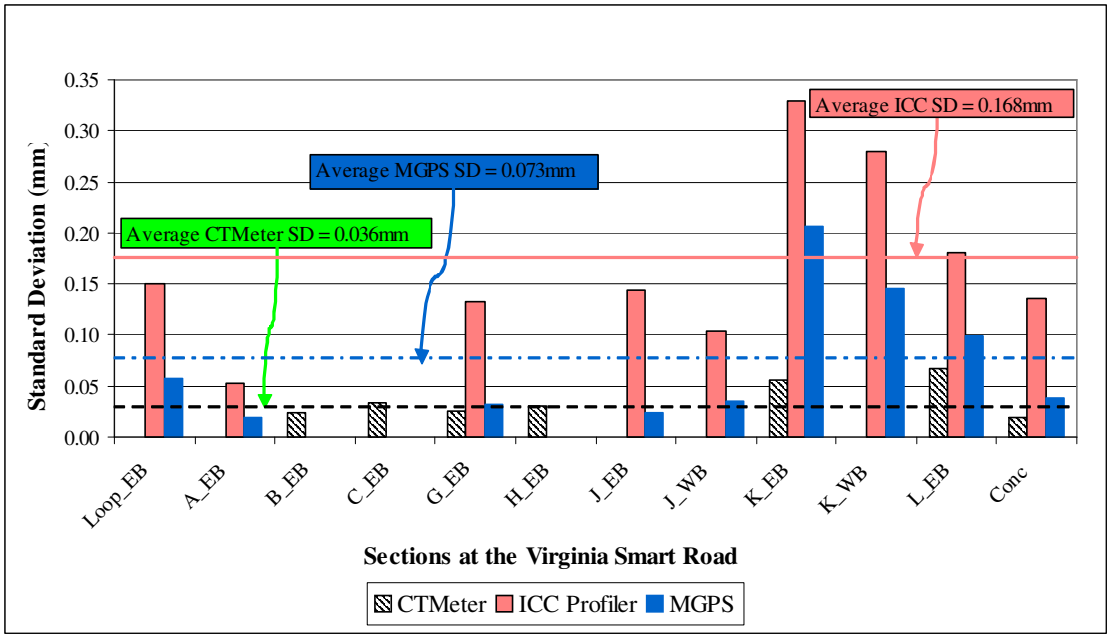

Figure 3-5 Coefficient of Variation of Laser-Based Macrotexture Measurements

3.2.3. Conclusion

For the surfaces investigated, the CTMeter appears to be the most repeatable system, followed by the MGPS system, and then the ICC profiler. However, since all three devices have relatively low standard deviation (lower than 0.17mm) and coefficient of variation (lower than 10%); they all may be considered repeatable measuring devices.

3.3. REGRESSION ANALYSIS BETWEEN LASER-BASED AND SAND PATCH MEASUREMENTS

The volumetric method is often considered as the "ground-truth" method for surface texture measurements. However, this method is time-consuming and operator-dependent. Hence, for standardization and convenience, it is important to find a more objective (e.g., laser-based) method that can replace the volumetric MTD as a representation of surfacemacrotexture. Therefore, MTD values obtained with Sand Patch were used as a reference and the correlations with the other three measures were investigated (detailed data presented in Appendix B).

3.3.1. Correlation between Laser-Based Measurements and Sand Patch MTD

Previous research suggested that the macrotexture measurements experienced more variation on the OGFC surface. Furthermore, there are some physical limitations associated with performing Sand Patch measurements on very porous surfaces. Hence, in order to investigate the effect of the OGFC surface on the correlation between the laser-based devices and Sand Patch, correlation analyses on all surfaces including and excluding the OGFC surface were conducted. Furthermore, in order to evaluate the effects of the various outputs from the CTMeter on the correlation with Sand Patch, the correlation analyses included RMS, Longitudinal MPD, and Transversal MPD. Linear regression analyses are presented in Appendix C and summarized in Table 3-2. Of the three laser-based devices, the CTMeter has the highest correlation (and smallest standard error) with the Sand Patch, followed by the MGPS system.

Table 3-2 Correlation between Laser-Based and Sand Patch Measurements

Device	Type of Measure	All Surfaces Included			OGFC Excluded		
		R^2	StdErr	No. of obsv	R^2	StdErr	No. of obsv
CTMeter	MPD	0.943	0.176	38	0.833	0.111	29
	RMS	0.923	0.198	38	0.752	0.135	29
	Long. MPD	0.940	0.180	38	0.735	0.140	29
	Tran. MPD	0.868	0.268	38	0.859	0.102	29
ICC Profiler	ICCTEX	0.884	0.251	38	0.792	0.124	29
MGPS	MPD	0.927	0.199	38	0.796	0.123	29

In general, the CTMeter MPD values correlate better with the MTD than the CTM RMS. The average MPD of all eight segments correlates better with Sand Patch than the average of the longitudinal or transversal segments.

The relatively higher values of macrotexture measurements on the OGFC surface contribute to higher correlation coefficients between the laser-based measurements and the Sand Patch MTD, but also to higher standard errors. Hence, the effect of the OGFC surface should be taken into consideration in the following sections.

The very high correlations observed between the laser-based measurements and Sand Patch MTD suggests that laser-based method could replace the Sand Patch for characterizing pavement surface macrotexture.

3.3.2. Conversion Equations

Since different devices usually give different results even measuring the same texture, it is important and useful to harmonize the measurements obtained with different texture measure devices. Since the Sand Patch test is generally considered a ground truth method for macrotexture measurement, and this test correlates well with other methods, it was used as reference to convert all the measurements obtained with the laser-based devices. Because of previously reported difficulties measuring texture on the OGFC, the harmonizing process has been conducted using all surfaces, and excluding the OGFC.

The conversion coefficients were determined using linear regression. Since the average MPD outputs of all eight segments have the highest correlation coefficient among the various CTMeter outputs with Sand Patch, also with the smallest standard error, hence, only the CTM_MPD outputs were considered. The following model was used for all the devices:

$$MTD_{SP} = y_0 + a * MPD_{Laser-Based} + \varepsilon \qquad (3.2)$$

where,
y_0 = The intercept parameter, and
a = The slope parameter of the first order polynomial
ε = Error

Table 3-3 summarized the conversion coefficients for both conditions at the Virginia Smart Road: using all surfaces and excluding the OGFC. Since the volumetric patch test can not be used to measure texture depths lower than 0.25mm, certain limits for application of these conversion equations should be set. Also, the highest Sand Patch MTD is used to get an upper limit. Consequently, the following ranges of application were determined for the conversion equations:

- CTMeter: 0.22mm ≤ MPD ≤ 3.14mm for all surfaces included model and 0.15mm ≤ MPD ≤ 1.55mm for OGFC excluded model,
- ICC profiler: 0.81mm ≤ ICCTEX ≤ 4.49mm for all surfaces included model and 0.47mm ≤ ICCTEX ≤ 2.92mm for OGFC excluded model, and
- MGPS: 0.37mm ≤ MPD ≤ 3.08mmfor all surfaces included model and 0.39mm ≤ MPD ≤ 1.52mm for OGFC excluded model

Table 3-3 Conversion Coefficients Based on the Virginia Smart Road Measurements

Model	Device	Type of Measure	y_0	a	R^2	StdErr
All Surfaces Included	CTMeter	MPD	0.036	0.982	0.943	0.176
	ICC Profiler	ICCTEX	-0.379	0.780	0.884	0.251
	MGPS	MPD	-0.148	1.062	0.927	0.199
OGFC Excluded	CTMeter	MPD	0.130	0.815	0.833	0.111
	ICC Profiler	ICCTEX	0.034	0.465	0.792	0.124
	MGPS	MPD	-0.138	1.007	0.797	0.123

Table 3-4 summarized the ranges for the ratio between the predicted and measured MTD based on the measurements obtained with the three devices using both models. The predicted MTD are very close to those measured using the Sand Patch. Although the models using all surfaces have higher R^2, they also result in a considerable higher standard error than those produced by the models excluding the OGFC. The higher coefficient of correlation may be explained by the wider range of textures considered in the case of the models including the OGFC. A comparison of the predicting capabilities of the two models is presented in the Chapter Four.

Table 3-4 Ratio of Predicted to Measured MTD for the Two Models

Model	Device	Type of Measure	Minimum	Maximum	Mean Value	No. of Obsv
All Surfaces Included	CTMeter	MPD	0.73	1.50	1.01	38
	ICC Profiler	ICCTEX	0.63	1.61	1.00	38
	MGPS	MPD	0.74	1.43	1.04	38
OGFC Excluded	CTMeter	MPD	0.78	1.38	1.01	29
	ICC Profiler	ICCTEX	0.76	1.25	1.02	29
	MGPS	MPD	0.75	1.36	1.02	29

3.4. CORRELATIONS BETWEEN LASER-BASED MEASUREMENTS

In this step, each measurement (Y) obtained with a laser-based device was correlated to all the others (X) using linear regression. Furthermore, the effect of the various factors on the correlation was investigated to achieve the following secondary objectives:

- To determine which of the various outputs from the CTMeter (MPD & RMS) correlates better with the other devices,
- To determine which of the segmental MPD outputs from the CTMeter [Average MPD of all segments, transversal segments (C&G) and longitudinal segments (A&E)] correlates best with the other devices,
- To determine whether texture convexity affects the correlations between the devices, and
- To determine whether surface mix type affects the correlations between the devices.

The regression analyses were conducted using all the data concurrently and then breaking them down by texture convexity and surface mix types.

3.4.1. Correlation Analyses Using All Sections

The texture measurements obtained with the laser-based devices were correlated with each other regardless of the type of surface mix or the feature of the surface. The various linear regression analyses are presented in Appendix C and summarized in Table 3-5. The following conclusions can be drawn from this table:

- The measurements obtained with the CTMeter and MGPS system have the best correlation, followed by the correlation between the CTMeter and ICC, then by the ICC and MGPS.
- As expected, the MPD output from the CTMeter correlates better with the measurements obtained with the other two devices than its RMS output.
- The average MPD output of all eight CTMeter segments correlates slightly better with the measurements obtained with the other two devices than the average of the transversal segments or longitudinal segments.

Table 3-5 Correlation Analyses between Laser-Based Measurements on the Virginia Smart Road

X/Y	ICC			MGPS		
	R^2	StdErr	No. of Obsv	R^2	StdErr	No. of Obsv
CTM_MPD	0.909	0.276	54	0.964	0.134	54
CTM_Tran	0.845	0.361	54	0.916	0.203	54
CTM_Long	0.883	0.314	54	0.931	0.184	54
CTM_RMS	0.863	0.339	54	0.908	0.212	54
ICC				0.879	0.243	54
MGPS	0.879	0.319	54			

3.4.2. Texture Convexity Effect

Comparison of the MPD and the RMS for a surface provides information on the nature of the texture convexity, that is, whether the texture orientation is positive, negative or neutral. In this step, the measurements obtained with the various laser-based devices

were correlated to each other separated by texture convexity. The various linear regression analyses, presented in Appendix C and summarized in Table 3-6, yielded the following conclusions:

- Regardless of the texture convexity, the measurements obtained with the CTMeter and the MGPS system have the best correlation.
- Regardless of the texture convexity, the MPD output from the CTMeter correlates better with the other two devices than its RMS output. In the case of the pavements with neutral texture, the MPD and RMS are very similar and thus provide similar coefficient of determination.
- Generally the three devices correlate better with each other on positive or negative texture than on neutral texture. However, this is probably due to the fact that the range of texture for the neutral group is narrower than for the other two groups.

Table 3-6 Correlation Analyses between Laser-Based Measurements Separated by Texture Convexity

Texture Convexity	X/Y	ICC			MGPS		
		R^2	StdErr	No. of Obsv	R^2	StdErr	No. of Obsv
Positive	CTM_MPD	0.925	0.239	28	0.970	0.117	28
	CTM_RMS	0.919	0.248	28	0.952	0.147	28
	ICC				0.907	0.204	28
	MGPS	0.907	0.265	28			
Negative	CTM_MPD	0.911	0.271	18	0.971	0.134	18
	CTM_RMS	0.906	0.279	18	0.944	0.188	18
	ICC				0.872	0.284	18
	MGPS	0.872	0.326	18			
Neutral	CTM_MPD	0.878	0.324	8	0.945	0.143	8
	CTM_RMS	0.880	0.322	8	0.943	0.145	8
	ICC				0.881	0.210	8
	MGPS	0.881	0.321	8			

In order to determine whether the differences between the various correlation coefficients (R^2) on different texture convexity are significant, the Analysis of Variation (ANOVA) presented in Table 3-7 was conducted. Only the CTM_MPD was used for analysis among the various outputs from the CTMeter.

Table 3-7 ANOVA Table for Texture Convexity

Source of Variation	SS	df	MS	F	P-value	F crit
Devices	0.00928	2	0.00464	27.6336	0.005	6.94428
Texture Convexity	0.00160	2	0.00080	4.75203	0.088	6.94428
Error	0.00067	4	0.00017			
Total	0.01154	8				

The ANOVA indicates that the correlations between different devices are significantly different for a 95% level of significance. Furthermore, the Tukey method suggested that the correlation between the CTMeter and MPGS system is significantly better than that between the CTMeter and ICC profiler or that between the ICC profiler and MGPS system. It is important to note that the P-value for Texture Convexity is 0.088, quite close to 0.05, indicating the differences for R^2 on different texture convexity are almost significantly different.

3.4.3. Surface Mix Effect

The macrotexture measurements analyzed were collected on four significantly different types of surface mixes, including:

- Stone Mastic Asphalt (SMA): Loop and Section L,
- Dense Asphalt: Section A, G, and J,
- Open-Graded Friction Course (OGFC): Section K, and
- Concrete Section.

In this step, the macrotexture measurements obtained with the laser-based devices on each type of surface were correlated to each other separately. The various linear regression analyses are presented in Appendix C and summarized in Table 3-8.

As expected, the R^2 for the various comparisons are lower than those in the previous cases because the range of texture for each mix is significantly narrowed than for all mixes combined. From the table, the following conclusions were drawn:

- The MPD output from the CTMeter generally correlates better with the MGPS system than the RMS output.
- The MPD output from the CTMeter correlates better with the ICC profiler on the Dense Asphalt surface and OGFC than the RMS output, but not on the SMA or the Concrete surfaces.
- On the OGFC section, the correlation coefficient between the CTMeter and the MGPS system is much higher than that between either of them and the ICC profiler.
- The MGPS measurements correlate better with the ICC measurements on the SMA or Concrete surfaces than on the other two surfaces.
- On the Concrete section, the CTMeter longitudinal MPD outputs have very low correlation coefficient with the measurements from the other two devices because this section is transversally grooved.

Table 3-8 Correlation Analyses between Laser-Based Measurements Separated by Surface Mix Types

Surface Mix Type	X/Y	ICC			MGPS		
		R^2	StdErr	No. of Obsv	R^2	StdErr	No. of Obsv
SMA	CTM_MPD	0.6202	0.215	12	0.522	0.111	12
	CTM_RMS	0.6876	0.195	12	0.5368	0.110	12
	ICC				0.8417	0.064	12
	MGPS	0.8417	0.139	12			
Dense-Asphalt	CTM_MPD	0.7292	0.101	24	0.7142	0.058	24
	CTM_RMS	0.6286	0.119	24	0.375	0.086	24
	ICC				0.3674	0.086	24
	MGPS	0.3674	0.155	24			
OGFC	CTM_MPD	0.4728	0.352	12	0.8934	0.213	12
	CTM_RMS	0.2233	0.428	12	0.6939	0.362	12
	ICC				0.5426	0.442	12
	MGPS	0.5426	0.328				
Concrete	CTM_MPD	0.6982	0.174	6	0.7295	0.045	6
	CTM_Tran	0.604	0.200	6	0.655	0.051	6
	CTM_Long	0.1056	0.300	6	0.2096	0.077	6
	CTM_RMS	0.7537	0.158	6	0.6426	0.052	6
	ICC				0.8833	0.030	6
	MGPS	0.8833	0.109	6			

CHAPTER 4
CONVERSION MODELS VALIDATION

In this chapter, three additional macrotexture measurements data sets were used to test the two sets of models developed in Chapter Three (summarized in Table 4-1), and to select the one that provides best overall prediction capabilities. The data were collected at the Virginia Smart Road, on several newly constructed pavements throughout Virginia, and on airport pavements at Wallops flight facility, also in Virginia.

Table 4-1 Summary of MTD Prediction Models

Device	All Surfaces Included	OGFC Excluded
CTMeter	$MTD_{Predicted} = 0.9821*MPD_{CTM}+0.0362$ [0.22mm ≤ MPD_{CTM} ≤ 3.14mm]	$MTD_{Predicted} = 0.8147*MPD_{CTM}+0.1303$ [0.15mm ≤ MPD_{CTM} ≤ 1.55mm]
ICC Profiler	$MTD_{Predicted} = 0.7796*ICCTEX-0.3793$ [0.81mm ≤ ICCTEX ≤ 4.49mm]	$MTD_{Predicted} = 0.4646*ICCTEX+0.0342$ [0.47mm ≤ ICCTEX ≤ 2.92mm]
MGPS System	$MTD_{Predicted} = 1.0624*MPD_{MGPS}-0.1479$ [0.37mm ≤ MPD_{MGPS} ≤ 3.08mm]	$MTD_{Predicted} = 1.0073*MPD_{MGPS}-0.1383$ [0.39mm ≤ MPD_{MGPS} ≤ 1.52mm]

4.1. SECOND VIRGINIA SMART ROAD DATA ANALYSIS

The location of the macrotexture measurements collected on August 17, 2001 at the Virginia Smart Road is shown in Figure 4-1. Only data from the CTMeter and the ICC profiler were used in this case (detail data presented in Appendix D). Six CTMeter measurements were taken on each section, three on the LWP and three on the BWP, separated 77.5ft, 152.5ft and 227.5ft from the western end of each section. The ICC measurements on 1.5m (5ft) centered on the locations of the CTMeter tests were extracted for comparisons with CTMeter measurements.

For each section, average MPD on the LWP and BWP were used for MTD prediction. The MTD were predicted for each device using both models and compared with each other, as shown in Figure 4-2.

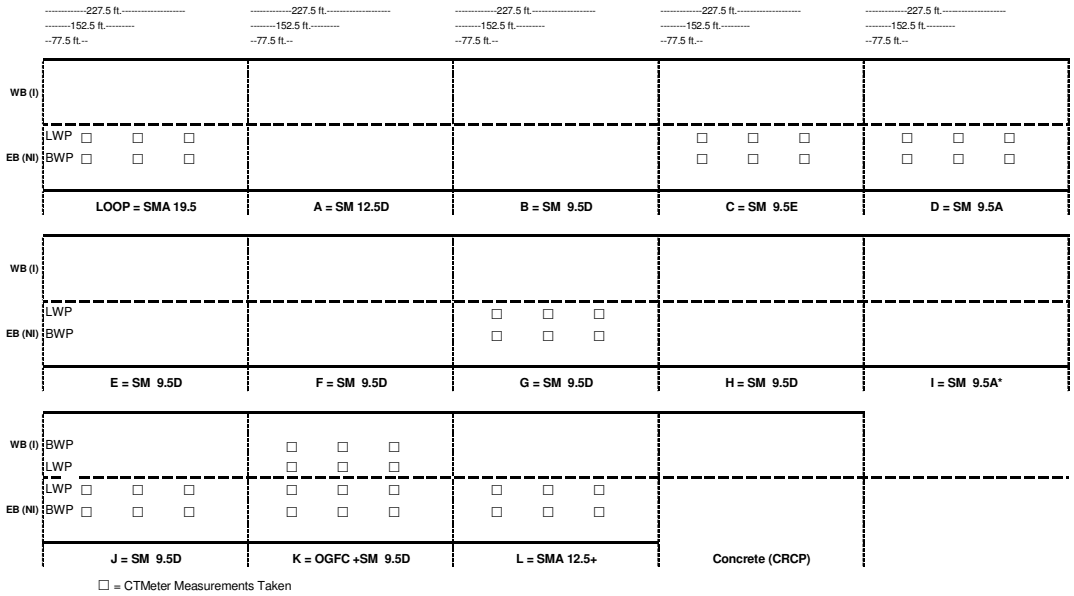

Figure 4-1 Locations of Measurements on Aug. 17, 2001 at the Virginia Smart Road

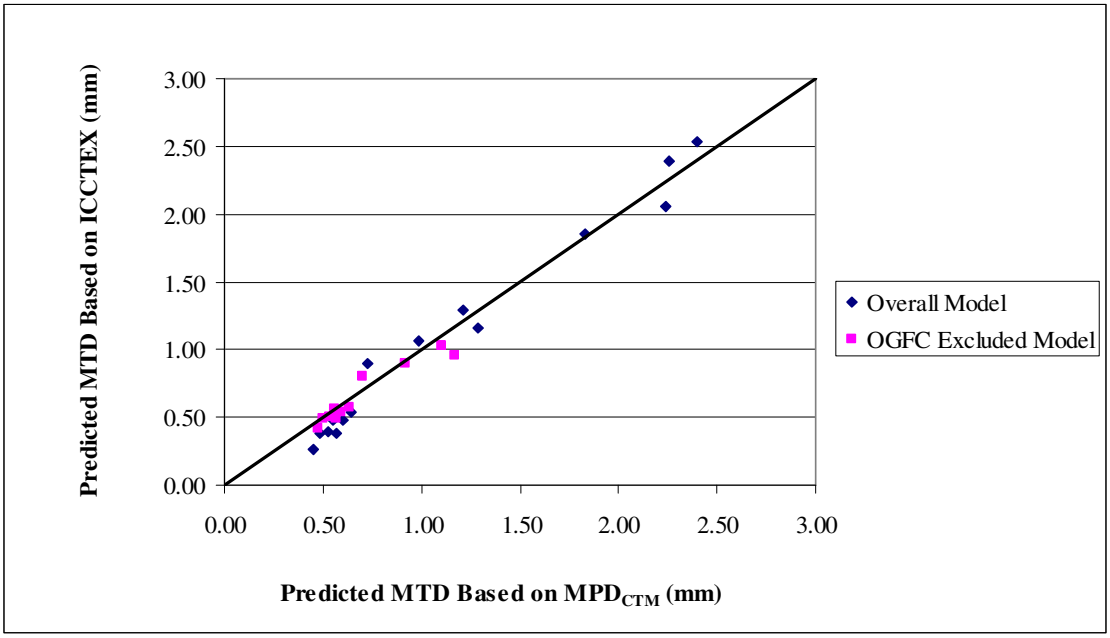

Figure 4-2 Comparison of MTD Predictions based on Average Macrotexture Measurements at the Virginia Smart Road

As expected, both models in general predict the same MTD for both devices. However, the MTD predicted using the OGFC-excluded models appear to match better than those using the Overall model. Paired t-tests indicate that for a 95% level of

significance the MTD predicted based on the MPD_{CTM} and the ICCTEX measurements are not significantly different for either model (Table 4-2).

Table 4-2 Comparison of Measured and Predicted MTD Based on Average Macrotexture Measurements at Virginia Smart Road

Statistics Parameter	Overall Model		OGFC Excluded Model	
	CTM Prediction	ICC Prediction	CTM Prediction	ICC Prediction
Mean	1.081	1.041	0.693	0.649
Variance	0.501	0.591	0.056	0.044
Observations	16	16	12	12
Pearson Correlation	0.989		0.957	
Hypothesized Mean Difference	0		0	
df	15		11	
t Stat	1.309		2.153	
P(T<=t) two-tail	0.210		0.054	
t Critical two-tail	2.131		2.201	

In general, the model validation based on the Virginia Smart Road measurements shows both models work well for MTD prediction. The predicted MTD based on different devices measurements are not statistically different for either model. However, it is important to note that this agreement was expected because most of the sections where this data set was collected are the same as those used for developing the models. Hence, data sets collected on other locations are necessary to further test the models and to select the most appropriate one.

4.2. NEWLY CONSTRUCTED HMA HIGHWAY PAVEMENTS

A second set of data was obtained from a selected sample of typical VDOT paving mixes, which were measured during the summer 2003. The ICC and CTMeter macrotexture data were collected on eight highway projects (summarized in Table 4-3), as part of a study to detect and quantify HMA segregation. There were 11 CTMeter measurements on the LWP and BWP for most projects, except the Project 02-1026 and 02-1039, which had only seven CTMeter measurements on each path. The ICC profiler measured the entire section of each project, but only the measurements overlapping the locations of the static measurements were extracted to compare with the CTMeter

measurements. It must be noted that it is possible that the two measurements were not perfectly overlapped for all the sections (detailed data presented in Appendix E).

Table 4-3 Test Site Locations

Project	Location	County	District	Mix
02-1026	I-81 Southbound from Woodstock	Shenandoah	Staunton	BM-25
02-1039	Rt. 7 West of Leesburg	Loudon	NOVA	SM-9.5 D
02-1041	Rt. 7 East of Berrysville	Frderick	Staunton	SM-12.5
02-1043	Rt. 15 East of Gordansville	Orange	Culpeper	SM-9.5
02-1050	Rt. 522 West of Rt 3 in Culpeper	Culpeper	Culpeper	BM-25
02-1056	Rt. 29 North of Danville	Pittsylvania	Lynchburg	IM-19.0
02-1068	Rt. 33 West of Elkton	Rockingham	Staunton	SM-12.5 A
02-1079	Rt. 460 East of Cedar Bluff	Tazewell	Bristol	SM-19.0

4.2.1. Model Validation Based on Individual Measurements

Figure 4-3 compares the MTD predicted based on the individual measurements collected on the LWP of the eight highway paving projects using both sets of models.

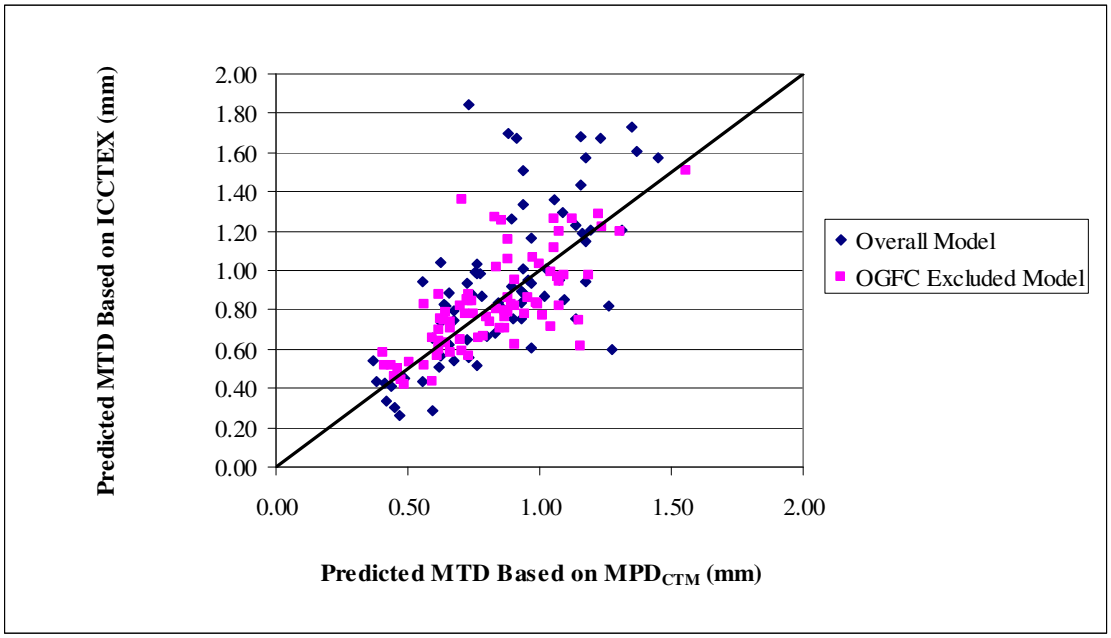

Figure 4-3 MTD Predictions Based on Individual ICCTEX Measurements on Highway Pavements

The figure suggests that, the overall model in general predicts significantly higher MTD based on the ICCTEX than on the MPD_{CTM}. The predicted MTD based on the ICCTEX and MPD_{CTM} are closer to each other using the OGFC excluded model than using the Overall model. Furthermore Paired t-tests for a 95% level of significance indicate that the predicted MTD based on the MPD_{CTM} and ICCTEX using the Overall model are significantly different, while those using the OGFC excluded model are not (Table 4-4).

Table 4-4 Comparison of Measured and Predicted MTD Predictions Based on Individual ICCTEX Measurements on Highway Surfaces

Statistics Parameter	Overall Model		OGFC Excluded Model	
	CTM Prediction	ICC Prediction	CTM Prediction	ICC Prediction
Mean	0.889	0.972	0.838	0.840
Variance	0.101	0.236	0.070	0.084
Observations	80	80	80	80
Pearson Correlation	0.790		0.790	
Hypothesized Mean Difference	0		0	
df	79		79	
t Stat	-2.440		-0.097	
P(T<=t) two-tail	0.017		0.923	
t Critical two-tail	1.990		1.990	

4.2.2. Model Validation Based on Average Measurements

Because it was not possible to exactly overlap the static and dynamic measurements in all sections, the average measurements on the LWP and BWP of each site were used for MTD prediction. Figure 4-4 compares the MTD predicted using both sets of models for the two devices.

Figure 4-4 suggests that the Overall model seems to over-predict the MTD computed based on the measurements of the ICC profiler. The OGFC-excluded models predicts rather close MTD values based on the MPD_{CTM} and ICCTEX, except at points A, B, and C. However, these locations have some special features that may explain this discrepancy. Point A had a localized area with particularly low CTMeter measurements. Points B and C correspond to measurements taken on heavily segregated areas.

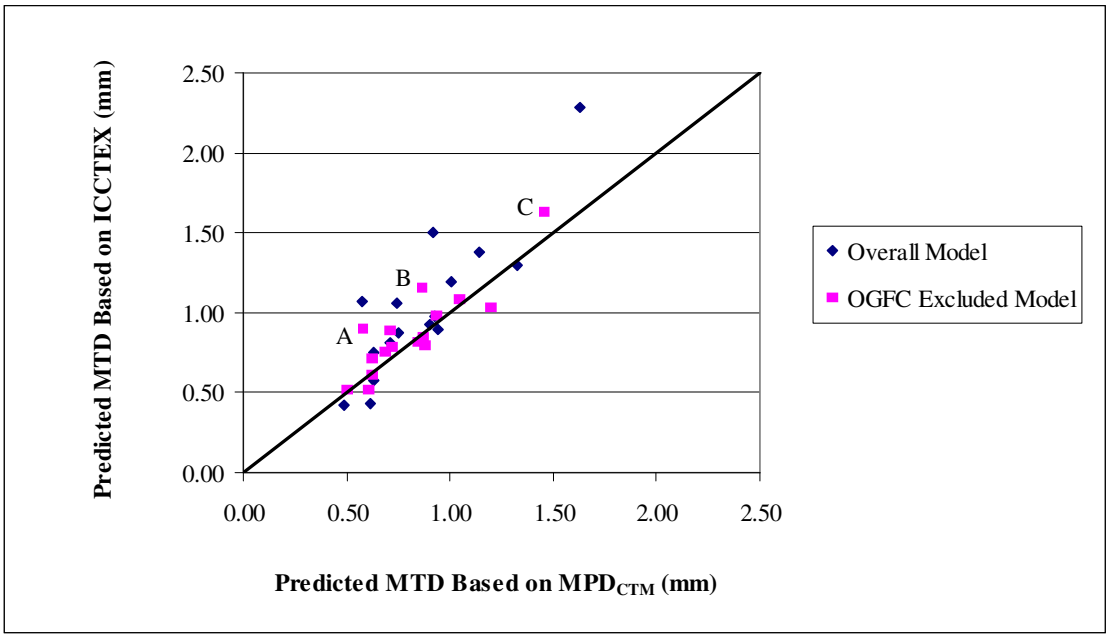

Figure 4-4 MTD Predictions Based on Average ICCTEX Measurements

Confirming the results of the previous section, paired t-tests for a 95% level of significance indicate that the predicted MTD based on the MPD_{CTM} and ICCTEX using the Overall model are significantly different, while those using the OGFC-excluded model are not (Table 4-5). Therefore, the conversion models excluding the OGFC have better prediction capabilities than those including the OGFC when used on standard roadway HMA mixes.

Table 4-5 Comparison of Measured and Predictions MTD Based on Average ICCTEX Measurements on Highway Surfaces

Statistics Parameter	Overall Model		OGFC Excluded Model	
	CTM Prediction	ICC Prediction	CTM Prediction	ICC Prediction
Mean	0.870	1.028	0.822	0.873
Variance	0.090	0.209	0.062	0.074
Observations	16	16	16	16
Pearson Correlation	0.870		0.870	
Hypothesized Mean Difference	0		0	
df	15		15	
t Stat	-2.571		-1.501	
P(T<=t) two-tail	0.021		0.154	
t Critical two-tail	2.131		2.131	

4.3. WALLOPS FLIGHT FACILITY

The Wallops flight facility is an active airport owned and operated by the National Aeronautics and Space Administration (NASA). Several test surfaces are distributed among three full-scale runways and numerous taxiways. These surfaces vary from grooved and non-grooved HMA and Portland Cement Concrete (PCC) to very smooth synthetic surfaces and numerous bituminous-based surface treatments. The test surfaces ranged in size from a 300 m (1,000 ft) long dense-graded asphalt concrete test section on a main runway to temporarily attached plates that were just over 1 m wide and less than 3 m long (4 by 8 ft). Table 4-6 lists the subsets of the surfaces available at Wallops that were used for this study (Yager, 2000). Three randomly selected locations were used for the static measurements on each section (detailed data presented in Appendix F).

Table 4-6 Evaluated Test Surfaces at Wallops

Surface Code	Width (m)	Length (m)	Surface Description
A	4.6	32.6	Non-grooved canvas belt-finished PCC
B	4.6	32.6	Grooved 1x1/4x1/4-inch canvas belt-finished PCC
C	4.6	32.6	Grooved 1x1/4x1/4-inch burlap drag-finished PCC
D	4.6	32.6	Non-grooved burlap drag-finished PCC
E	4.6	93.0	Non-grooved small-aggregate HMA
F	4.6	32.6	Grooved 2x1/4x1/4-inch small aggregate HMA
K	0.9	25.9	Driveway sealer without sand on K0
K0	0.9	25.9	Non-grooved float-finished PCC
S-0	1.2	18.6	Untreated area adjacent to skidabrader sites
S-1	1.2	18.6	Non-grooved PCC w/Skidabrader® light texture (1994)
S-2	1.2	18.6	Non-grooved PCC w/Skidabrader® medium texture (1994)
S-3	1.2	18.6	Non-grooved PCC w/Skidabrader® high texture (1994)
S-4	1.2	18.6	Non-grooved PCC w/Skidabrader® very high texture (1994)
S-5	1.2	83.5	Non-grooved PCC w/Skidabrader® medium texture (1995)
S-6	1.2	55.8	Non-grooved PCC w/Skidabrader® medium texture (1997)
MS/1	0.9	27.7	MS/0 with slurry seal overlay (1995)
MS/2	0.9	27.7	MS/0 with microsurface, single overlay (1995)
MS/3	0.9	27.7	MS/0 with microsurface, double oberlay (1995)
MS/4	0.9	27.7	MS/0 with anti-skid overlay (1999)

Data collected in 1998 and 1999 were used to test the MTD prediction models on a wide range of airport surfaces. This data included volumetric texture depth

measurements using glass beads by an experienced person from Pennsylvania State University (PSU) and CTMeter measurements. For each section, the averages of three measurements taken with each device were used. Figure 4-5 compares the MTD predicted based on the average CTMeter measurements for both models to the average measured MTD.

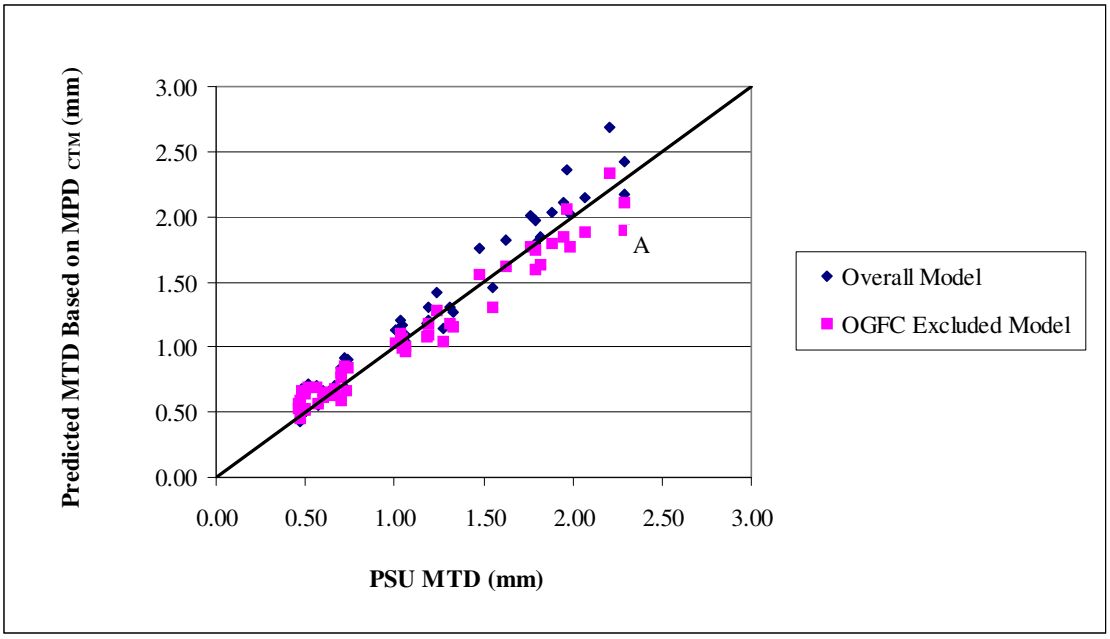

Figure 4-5 MTD Predictions Based on CTMeter Measurements on Airport Surfaces

Figure 4-5 suggests that, the CTMeter conversion model excluding the OGFC predicts MTD values that are very close to the measured MTD. The largest difference between the predicted and measured MTD is found at point A, which corresponds to a special Surface S-4 (Non-grooved PCC w/Skidabrader® with very high texture). The Overall model predictions are not as good as those using the OGFC-excluded model.

Consistently with the two previous comparisons, paired t-tests indicate that for a 95% level of significance the predicted MTD based on the MPD_{CTM} using the Overall model are significantly different from the PSU MTD, but the predictions using the OGFC-excluded model are not (Table 4-7). This supports the previous finding that the models excluding the OGFC should be used for general application.

Table 4-7 Comparison of Measured and Predicted MTD Based on CTMeter Measurements on Airport Surfaces

Statistics Parameter	Overall Model		OGFC Excluded Model	
	PSU MTD	CTM Prediction	PSU MTD	CTM Prediction
Mean	1.114	1.197	1.114	1.093
Variance	0.339	0.386	0.339	0.266
Observations	51	51	51	51
Pearson Correlation	0.982		0.982	
Hypothesized Mean Difference	0		0	
df	50		50	
t Stat	-4.903		1.192	
P(T<=t) two-tail	0.000		0.239	
t Critical two-tail	2.009		2.009	

4.4. SUMMARY

The model validation analysis indicates that the conversion models developed excluding the OGFC surface have better prediction capabilities than the overall models on non-porous surfaces. The MTD predictions based on the CTMeter and ICC measurements using the OGFC-excluded models are closer to each other than those using the overall models. Therefore, the conversion models excluding the OGFC should be used for general application on non-porous surfaces.

CHAPTER 5
FINDINGS, CONCLUSIONS, AND RECOMMENDATIONS

This thesis compared macrotexture measurements obtained using the volumetric method (Sand Patch) and three laser-based devices: MGPS system, ICC laser profiler, and Circular Texture Meter (CTMeter). The models were developed using measurements from the Virginia Smart Road. The developed models were verified using measurements at other highway and airport surfaces. The main findings and conclusions of the investigation are presented following.

5.1. FINDINGS

The following findings were obtained from the correlation analyses:

1. The three laser devices were found to have relatively low standard deviation (lower than 0.17mm) and coefficient of variation (lower than 10%). Hence, their repeatability was considered acceptable. The CTMeter appears to be the most repeatable of the three devices, followed by the MGPS System, and then the ICC profiler.
2. The output of the devices appears to be different. This is because of the different analytical approach used by the devices. However, they are all highly correlated with the Sand Patch MTD ($R^2 \geq 0.88$). The CTMeter MPD has the highest correlation with the Sand Patch MTD, followed by the MGPS system, and then the ICC profiler.
3. The convexity of the surface texture appears to have a moderate effect on the relationships among the laser-based measurements. Laser-based measurements correlate better on positive or negative textures than on the neutral textures.
4. The CTMeter MPD outputs correlate better with the other devices' macrotexture measurements than its RMS output. Furthermore, among the various CTMeter MPD outputs, the average MPD of all eight segments correlates better with the other devices' macrotexture measurements than the average MPD of Longitudinal or Transversal segments.

5.2. CONCLUSIONS

The very high coefficients of determination (R^2) between the laser-based macrotexture measurements and the Sand Patch MTD suggest the potential of using the laser-based macrotexture measurements in line of the traditional volumetric method for measuring surface macrotexture. The following models were developed to convert laser-based measurements to the volumetric MTD on non-porous surfaces.

CTMeter	$MTD_{Predicted} = 0.8147*MPD_{CTM}+0.1303$ $[0.15mm \leq MPD_{CTM} \leq 1.55mm]$
ICC Profiler	$MTD_{Predicted} = 0.4646*ICCTEX+0.0342$ $[0.47mm \leq ICCTEX \leq 2.92mm]$
MGPS System	$MTD_{Predicted} = 1.0073*MPD_{MGPS}-0.1383$ $[0.39mm \leq MPD_{MGPS} \leq 1.52mm]$

5.3. RECOMMENDATIONS

The models developed were based on measurements on a limited number of surface types. Testing on a wider range of surfaces is recommended for further calibration and validation of the conversion models.

REFERENCES

Abe, H., Tamai, A., Henry, J.J., and Wambold, J. (2000) ***"Measurement of Pavement Macrotexture with Circular Texture Meter,"*** Transportation Research Record 1764, pp 201-209. Transportation Research Board, Washington, DC.

Andresen, A., Lange, G., Holshagen, B., and Norheim, A. (2003) ***"Comparison of Pavement Texture Measuring Systems,"*** AVINOR Technical Report No.: OKK 2003-1, ISBN 82-91156-26-3.

ASTM (2003). ***"Wk364 Test Method for Measuring Pavement Texture Using an Outflow Meter,"*** http://www.astm.org/cgi-bin/SoftCart.exe/DATABASE.CART/WORKITEMS/ WK364.htm?E+mystore, 09/03/2003.

ASTM E 965 – 96, ***"Standard Test Method for Measuring Pavement Macrotexture Depth Using a Volumetric Technique,"*** Books of ASTM Standards, Vol. 4.03. ASTM International, West Conshohocken, PA.

ASTM E 1960 – 98, ***"Standard Practice for Calculating International Friction Index of a Pavement Surface,"*** Books of ASTM Standards, Vol. 4.03. ASTM International, West Conshohocken, PA.

ASTM E 2157 – 01, ***"Standard Test Method for Measuring Pavement Macrotexture Properties Using the Circular Track Meter,"*** Books of ASTM Standards, Vol. 4.03. ASTM International, West Conshohocken, PA.

Cross, S.A., and Brown, E.R. (1993) ***"Effect of Segregation on Performance of Hot-Mix Asphalt,"*** Transportation Research Record 1417, pp 117-126. Transportation Research Board, Washington, DC.

Davis, R.M., Flintsch, G.W., Al-Qadi, I.L., and McGhee, K.K. (2002) ***"Effect of Wearing Surface Characteristics on Measured Pavement Skid Resistance and Texture"*** (CR-ROM), 81st Meeting of the Transportation Research Board, Washington, DC.

Dupont, P., and Ganga, Y. (1995) ***"Skid Resistance and Texture of Road Surfaces on Difficult Sites,"*** Permanent International Association of Road Congresses (PIARC), Montreal 1995, pp 35-39. Individual Papers Committees and Working Groups.

Flintsch, G.W., De Leon, E.G., McGhee, K.K., and Al-Qadi, I.L (2003-a) ***"Pavement Surface Macrotexture – Measurement and Application,"*** Transportation Research Record 1060, pp 177-182. Transportation Research Board, Washington, DC.

Flintsch, G.W., McGhee, K.K., and de Leon, E. (2003-b) ***"Use of Surface Macrotexture Measurement to Detect Segregation,"*** Virginia Transportation Research Council Report VTRC 03-R12. VTRC, Charlottesville, Virginia.

Henry J. J. (2000). ***"NCHRP Synthesis 291 Evaluation of Pavement Friction Characteristics A Synthesis of Highway Practice."*** Transportation Research Board, Washington, DC.

International Standards Organization 13473-1 (1997), ***"Characterization of Pavement Texture by Use of Surface Profiles – Part 1: Determination of Mean Profile Depth",*** TC 43/SC 1. Geneva, Switzerland.

International Standards Organization 13473-2 (2002), "***Characterization of pavement texture by use of surface profiles -- Part 2: Terminology and basic requirements related to pavement texture profile analysis***", TC 43/SC 1. Geneva, Switzerland.

Jayawickrama, P.W., Prasanna, R. and Senadheera, S.P (1995), ***"Survey of State DOT Practices to Control Skid resistance on HMAC Surfaces."*** Transportation Research Record 1536, pp52-58. Transportation Research Board, Washington, DC.

Kandhal, P.S., and Parker F., JR. (1998) ***"NCHRP Report 405 Aggregate Tests Related to Asphalt Concrete Performance in Pavements."*** Transportation Research Board, Washington, DC.

Khedaywi, T.S., and White, T.D. (1996) ***"Effect of Segregation on Fatigue Performance of Asphalt Paving Mixture,"*** Transportation Research Record 1543, pp 63-70. Transportation Research Board, Washington, DC.

McGhee, K.K., and Flintsch, G.W. (2003) ***"High-Speed Texture Measurement of Pavements,"*** Virginia Transportation Research Council Report VTRC 03-R9. VTRC, Charlottesville, Virginia.

Nordic (1999) ***"Influence of Road Surface Texture on Traffic Characteristics,"*** Road & Transport Research, No 2 Http://www.vti.se/nordic/2-99mapp/299sw.html 8/25/2003.

Sandberg, U., and Ejsmont, J.A. (2002) ***Tyre/Road Noise Reference Book,*** Printed by MODENA in Poland, ISBN 91-631-2610-9, pp 89-93.

Sixbey, D.G. (1998) ***"It Takes More than Mirrors to See Your True Profile,"*** http://www.tfhrc.gov/pubrds/marapr98/profile.htm 08/16/2003.

Stroup-Gardiner, M., and Brown, E.R. (2000) ***"Segregation in Hot-Mix Asphalt Pavements,"*** NCHRP Report 441. Transportation Research Board, Washington, DC.

Wambold, J. C., Antle, C. E., Henry, J.J., and Rado, Z. (1995) ***"International PIARC Experiment to Compare and Harmonize Texture and Skid Resistance Measurements,"*** Final Report, May 1995.

Yager, T.J. (2000) ***"Seventh Annual Tire/Runway Friction Workshop: Summary and Proceedings Document,"*** NASA Langley Research Center, Hampton, Virginia.

APPENDIX A
DATA FOR REPEATABILITY ANALYSIS

Table A-1 Repeated CTMeter MPD Measurements at the Virginia Smart Road (mm)

Section	Point	1st Run	2nd Run	3rd Run
B&C	1	0.68	0.68	0.63
	2	0.61	0.62	0.6
	3	0.59	0.6	0.54
	4	0.59	0.68	0.6
	5	0.51	0.55	0.49
	6	0.61	0.64	0.65
G&H	1	0.48	0.48	0.46
	2	0.6	0.51	0.52
	3	0.45	0.45	0.42
	4	0.62	0.62	0.57
	5	0.54	0.63	0.59
	6	0.63	0.66	0.64
K&L	1	2.95	3.06	3
	2	2.17	2.27	2.32
	3	1.91	1.98	1.94
	4	0.88	1.01	0.96
	5	0.99	0.86	0.98
	6	0.8	0.89	0.77
Concrete	1	0.58	0.59	0.53
	2	0.44	0.44	0.42
	3	0.36	0.37	0.38
	4	0.65	0.7	0.68

Table A-2 Repeated ICC MPD and MGPS MPD Measurements at the Virginia Smart Road (mm)

Location		ICC Profiler MPD			MGPS MPD		
		1st pass	2nd pass	3rd pass	1st pass	2nd pass	3rd pass
Loop-EB	77.5', LWP	1.970	1.940	1.838	1.090	1.077	0.961
	77.5', BWP	2.374	2.344	2.493	1.359	1.269	1.316
	152.5', LWP	1.832	2.060	1.560	0.950	1.015	0.922
	152.5', BWP	2.054	1.865	1.413	0.974	0.989	0.978
	227.5', LWP	1.764	1.738	1.826	0.977	0.953	1.109
	227.5', BWP	1.970	2.215	2.179	1.351	1.248	1.166
A-EB	77.5', LWP	0.830	0.794	0.863	0.549	0.529	0.512
	77.5', BWP	0.850	0.902	0.835	0.525	0.523	0.511
	152.5', LWP	0.942	0.840	0.928	0.618	0.579	0.599
	152.5', BWP	0.946	0.924	0.986	0.550	0.535	0.553
	227.5', LWP	0.916	0.804	0.800	0.535	0.547	0.573
	227.5', BWP	1.030	0.854	0.976	0.506	0.505	0.569
G-EB	77.5', LWP	1.036	1.000	1.144	0.749	0.717	0.641
	77.5', BWP	1.215	1.090	1.212	0.634	0.585	0.568
	152.5', LWP	1.126	1.371	0.925	0.744	0.783	0.739
	152.5', BWP	1.278	1.431	1.012	0.636	0.633	0.612
	227.5', LWP	0.958	1.004	1.028	0.638	0.693	0.736
	227.5', BWP	1.028	1.350	1.052	0.605	0.627	0.612
J-EB	77.5', LWP	1.152	1.042	0.802	0.697	0.729	0.722
	77.5', BWP	1.186	1.353	0.988	0.822	0.863	0.797
	152.5', LWP	0.986	1.293	1.203	0.670	0.696	0.637
	152.5', BWP	1.134	1.060	0.880	0.881	0.911	0.886
	227.5', LWP	1.046	1.090	1.024	0.709	0.653	0.709
	227.5', BWP	1.379	1.048	1.087	0.772	0.786	0.746
K-EB	77.5', LWP	3.658	3.458	3.447	3.715	3.340	3.288
	77.5', BWP	3.317	5.221	4.374	3.094	3.166	3.842
	152.5', LWP	2.611	2.581	3.040	1.717	1.904	1.756
	152.5', BWP	3.341	2.874	3.066	2.101	2.062	2.303
	227.5', LWP	3.167	3.369	2.922	1.808	1.809	1.619
	227.5', BWP	3.339	2.996	3.054	1.807	1.847	2.270
L-EB	77.5', LWP	1.784	0.982	1.506	0.948	0.762	0.894
	77.5', BWP	1.952	2.227	2.126	1.057	1.132	1.023
	152.5', LWP	1.685	1.572	1.596	0.978	1.104	0.907
	152.5', BWP	2.407	2.554	2.584	1.188	1.102	1.420
	227.5', LWP	1.647	1.663	1.979	0.949	0.983	0.937
	227.5', BWP	2.141	2.321	2.527	1.322	1.159	1.461
Conc.	77.5', LWP	1.614	1.724	1.989	0.852	0.873	0.901
	77.5', BWP	1.557	1.439	1.328	0.784	0.806	0.808
	152.5', LWP	0.892	1.178	1.093	0.696	0.698	0.638
	152.5', BWP	0.832	1.127	1.186	0.819	0.711	0.674
	227.5', LWP	1.227	1.223	1.093	0.673	0.699	0.804
	227.5', BWP	1.062	1.239	1.215	0.677	0.675	0.702
K-WB	77.5', LWP	2.769	2.800	2.877	1.663	1.707	1.497
	77.5', BWP	3.143	4.958	2.994	2.005	2.757	2.578
	152.5', LWP	2.644	2.675	2.800	1.727	1.667	1.715
	152.5', BWP	3.477	3.943	3.537	1.838	2.089	2.084
	227.5', LWP	3.212	3.227	3.177	2.086	1.877	1.959
	227.5', BWP	2.943	3.024	3.259	2.534	2.712	2.666
J-WB	77.5', LWP	1.078	1.048	1.257	0.650	0.650	0.605
	77.5', BWP	1.281	1.198	1.251	0.782	0.875	0.794
	152.5', LWP	1.169	1.296	1.269	0.708	0.677	0.678
	152.5', BWP	1.482	1.418	1.611	0.740	0.737	0.767
	227.5', LWP	1.239	1.205	1.455	0.692	0.668	0.780
	227.5', BWP	1.461	1.523	1.784	0.880	0.791	0.825

APPENDIX B
MACROTEXTURE MEASUREMENTS AT THE VIRGINIA SMART ROAD ON APRIL, 9 2002

Table B-1 Macrotexture measurements at the Virginia Smart Road on April, 9 2002 Unit: mm)

Site	Location	Sand Patch	CTM MPD	CTM_Long.	CTM RMS	CTM_Trans.	ICC Texture	MGPS
Loop-EB	77.5', LWP	0.97	1.11	1.07	1.17	1.15	1.92	1.04
	77.5', BWP	1.39	1.23	1.04	1.16	1.26	2.4	1.31
	152.5', LWP	0.73	1.08	0.81	0.82	0.65	1.82	0.96
	152.5', BWP	1.13	1.07	0.94	1.01	1.15	1.78	0.98
	227.5', LWP	0.89	0.99	1.09	0.94	0.84	1.78	1.01
	227.5', BWP	1.29	1.11	1.01	0.96	1.44	2.12	1.26
A-EB	77.5', LWP	0.4	0.26	0.27	0.25	0.26	0.83	0.53
	77.5', BWP	0.46	0.32	0.24	0.29	0.31	0.86	0.52
	152.5', LWP	0.4	0.33	0.32	0.46	0.33	0.9	0.6
	152.5', BWP		0.4	0.36	0.33	0.35	0.95	0.55
	227.5', LWP	0.34	0.24	0.28	0.21	0.23	0.84	0.55
	227.5', BWP	0.39	0.29	0.29	0.31	0.26	0.95	0.53
G-EB	77.5', LWP	0.56	0.59	0.69	0.56	0.55	1.06	0.7
	77.5', BWP		0.49	0.4	0.43	0.56	1.17	0.6
	152.5', LWP	0.56	0.56	0.63	0.46	0.51	1.14	0.76
	152.5', BWP		0.59	0.61	0.51	0.7	1.24	0.63
	227.5', LWP	0.48	0.47	0.49	0.35	0.41	1	0.69
	227.5', BWP		0.55	0.54	0.44	0.46	1.14	0.61
J-EB	77.5', LWP	0.54	0.53	0.46	0.45	0.58	1	0.72
	77.5', BWP		0.61	0.6	0.51	0.69	1.18	0.83
	152.5', LWP	0.54	0.53	0.56	0.46	0.48	1.16	0.67
	152.5', BWP		0.65	0.7	0.55	0.65	1.02	0.89
	227.5', LWP	0.6	0.61	0.51	0.53	0.69	1.05	0.69
	227.5', BWP		0.64	0.67	0.5	0.7	1.17	0.77
J-WB	77.5', LWP		0.51	0.55	0.64	0.62	1.13	0.64
	77.5', BWP	0.71	0.7	0.86	0.83	0.63	1.24	0.82
	152.5', LWP		0.57	0.53	0.88	0.56	1.24	0.69
	152.5', BWP	0.74	0.78	0.57	0.92	0.81	1.5	0.75
	227.5', LWP		0.61	0.53	0.8	0.8	1.3	0.71
	227.5', BWP	0.79	0.75	0.79	0.68	0.79	1.59	0.83
L-EB	77.5', LWP	0.61	0.63	0.68	0.59	0.58	1.42	0.87
	77.5', BWP	0.99	0.92	0.89	0.92	0.87	2.1	1.07
	152.5', LWP	0.64	0.78	0.59	0.73	0.94	1.62	1
	152.5', BWP	1.02	1.16	1.18	1.2	1.14	2.52	1.24
	227.5', LWP	0.71	0.79	0.65	0.75	0.76	1.76	0.96
	227.5', BWP	0.89	1.09	1.02	1.08	0.87	2.33	1.31
K-EB	77.5', LWP	3.12	3.15	2.88	3.41	3.41	3.52	3.45
	77.5', BWP		3.12	3.04	2.65	3.24	4.3	3.37
	152.5', LWP	2.09	1.69	1.82	1.68	1.82	2.74	1.79
	152.5', BWP		2.04	1.88	2.01	2.37	3.09	2.16
	227.5', LWP	2.32	1.93	2.17	1.78	1.8	3.15	1.75
	227.5', BWP		1.82	2.32	1.49	1.6	3.13	1.97
K-WB	77.5', LWP	2.02	1.66	1.63	2.09	1.41	2.82	1.62
	77.5', BWP	2.34	2.17	1.91	2.28	3.66	3.7	2.45
	152.5', LWP	1.68	1.78	1.58	2.09	1.54	2.71	1.7
	152.5', BWP	2.24	2.05	1.89	1.98	1.8	3.65	2
	227.5', LWP	2.06	2.37	2.3	2.33	2.48	3.21	1.97
	227.5', BWP	2.46	2.78	2.66	2.5	2.58	3.08	2.64
Conc.	77.5', LWP	0.82	0.91	0.76	1.14	1.03	1.78	0.88
	77.5', BWP		0.88	0.87	0.99	0.84	1.44	0.8
	152.5', LWP	0.56	0.61	0.8	0.74	0.58	1.05	0.68
	152.5', BWP		0.64	0.72	0.74	0.72	1.05	0.73
	227.5', LWP	0.68	0.49	0.58	0.57	0.36	1.18	0.73
	227.5', BWP		0.58	0.53	0.81	0.58	1.17	0.68

APPENDIX C
LINEAR REGRESSION ANALYSES FOR DATA SET COLLECTED ON APRIL 9, 2002 AT THE VIRGINIA SMART ROAD

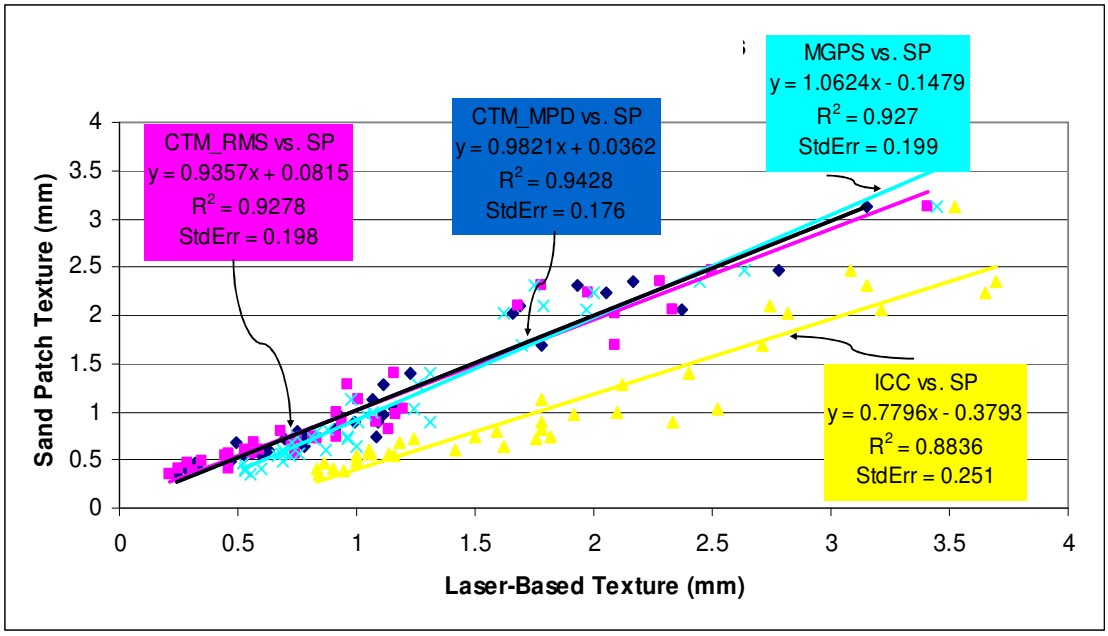

Figure C-1 Correlations between Sand Patch MTD and Laser-Based Macrotexture Measurements on All the Smart Road Surfaces

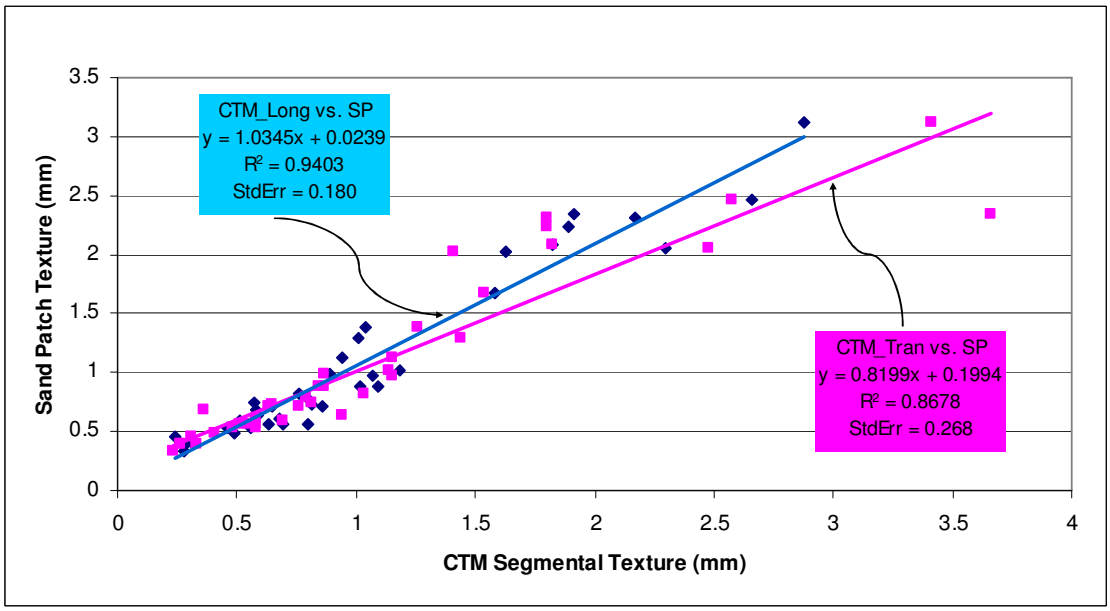

Note: A&E: Longitudinal Segments, C&G: Transversal Segments

Figure C-2 Correlations between Sand Patch MTD and CTMeter Segmental MPD on All the Smart Road Surfaces

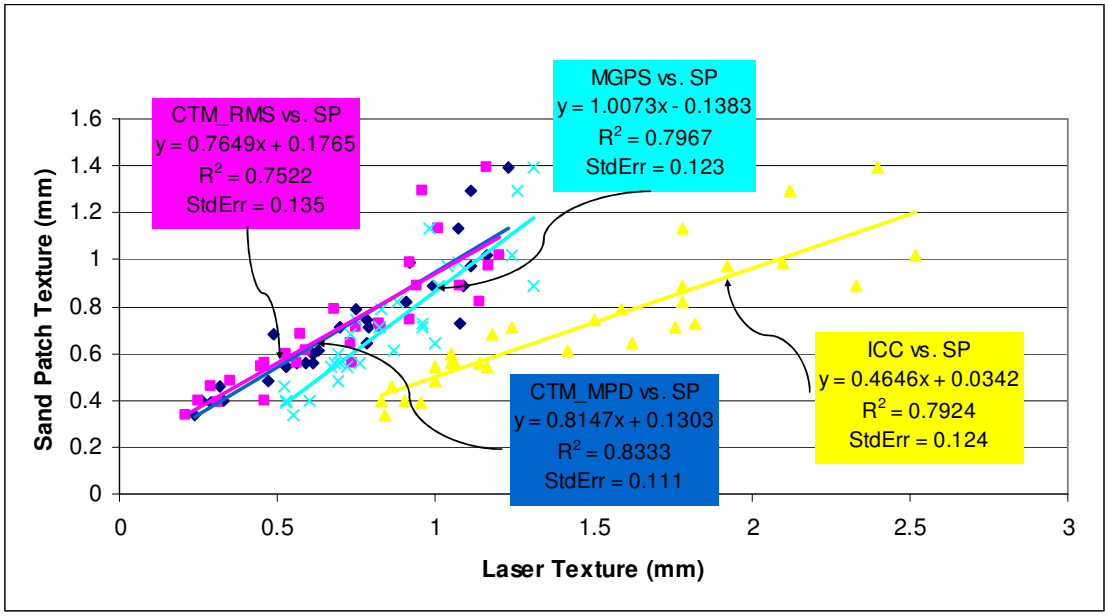

Figure C-3 Correlations between Sand Patch MTD and Laser-Based Measurements on Surfaces Excluding the OGFC

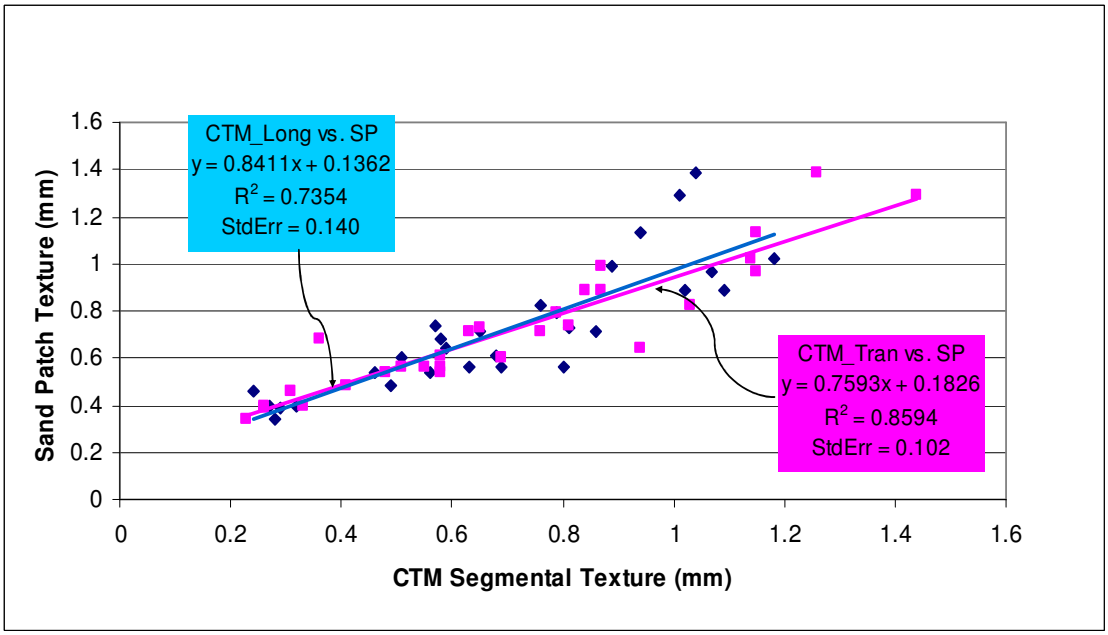

Figure C-4 Correlations between the Sand Patch MTD and CTMeter Segmental MPD on Surfaces Excluding the OGFC

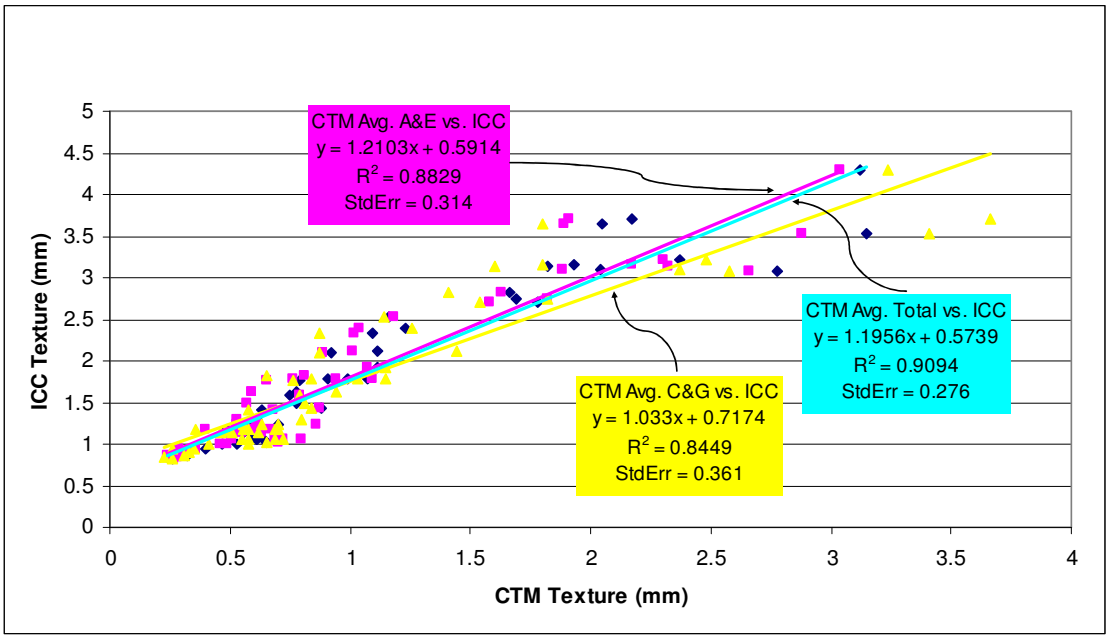

Figure C-5 Correlations between ICCTEX and CTM Segmental MPD on All the Smart Road Surfaces

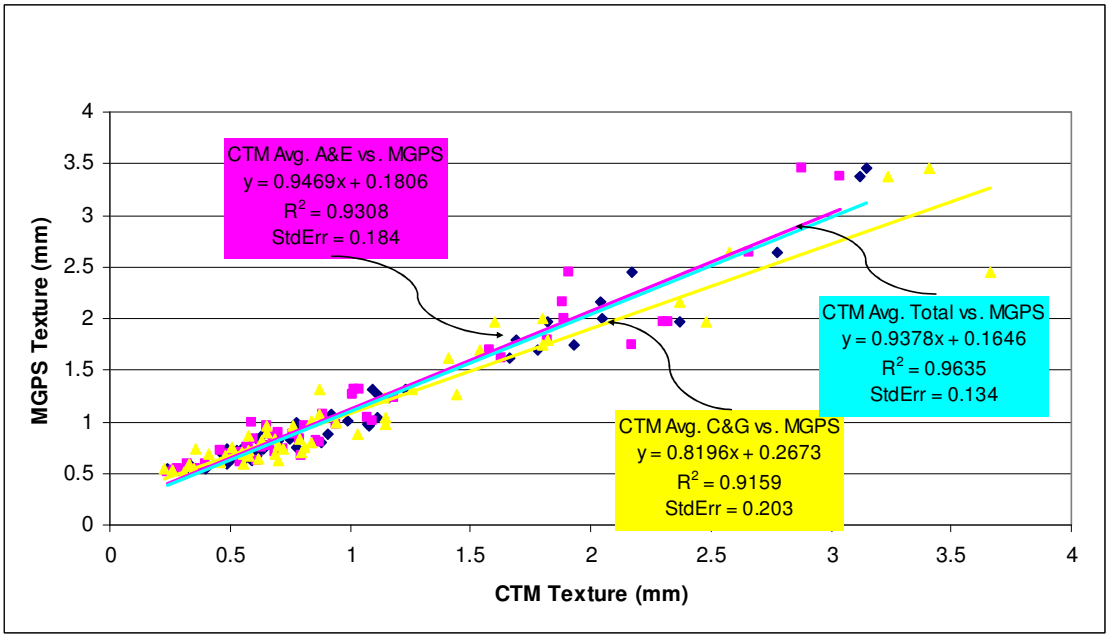

Figure C-6 Correlations between MGPS MPD and CTM Segmental MPD on All the Smart Road Surfaces

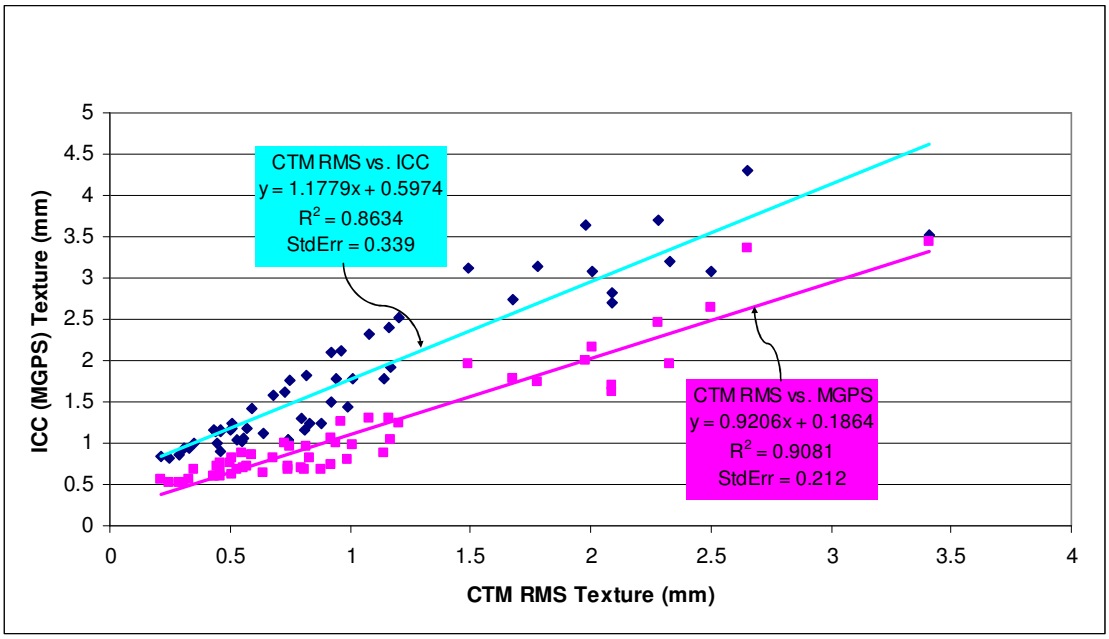

Figure C-7 Correlation between ICCTEX (MGPS MPD) and CTM RMS on All the Smart Road Surfaces

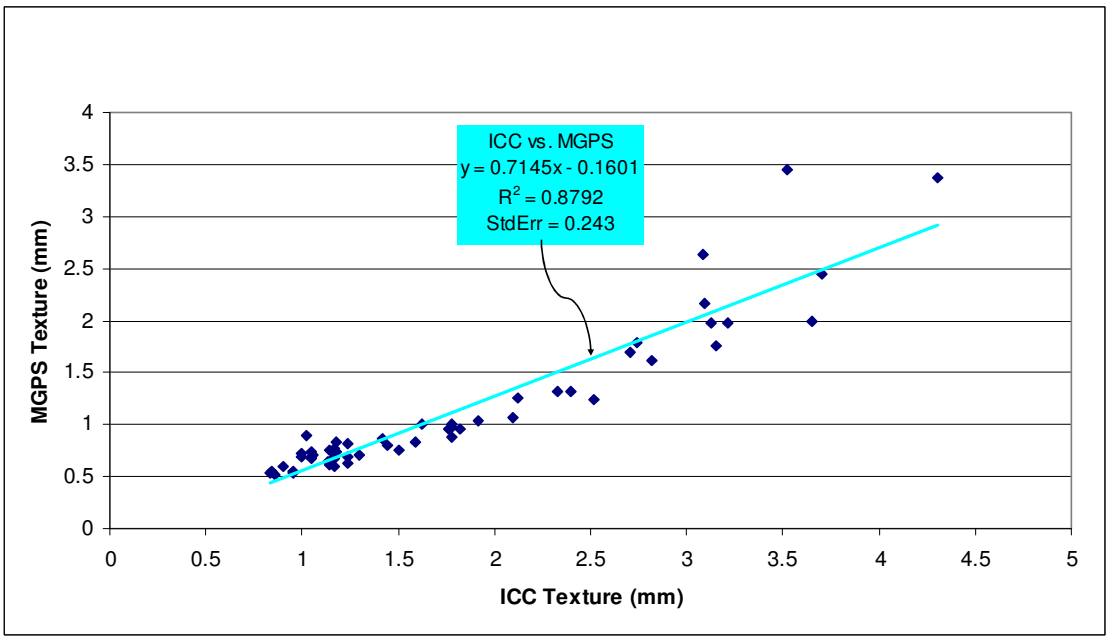

Figure C-8 Correlation between MGPS MPD and ICCTEX on All the Smart Road Surfaces

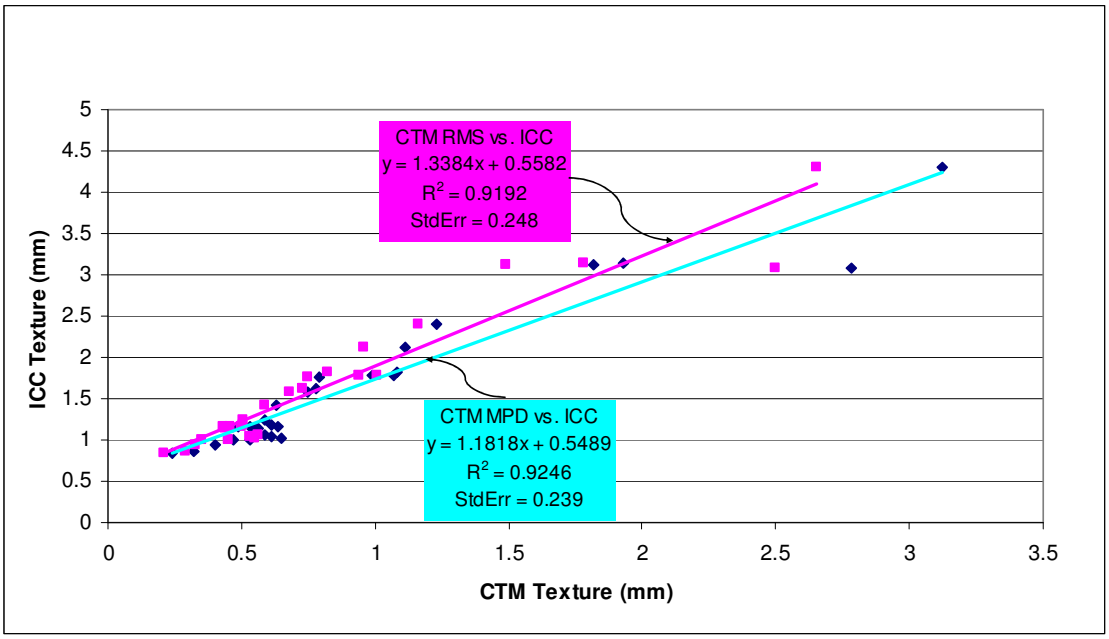

Figure C-9 Correlations between ICCTEX and CTM Texture on Positive Texture

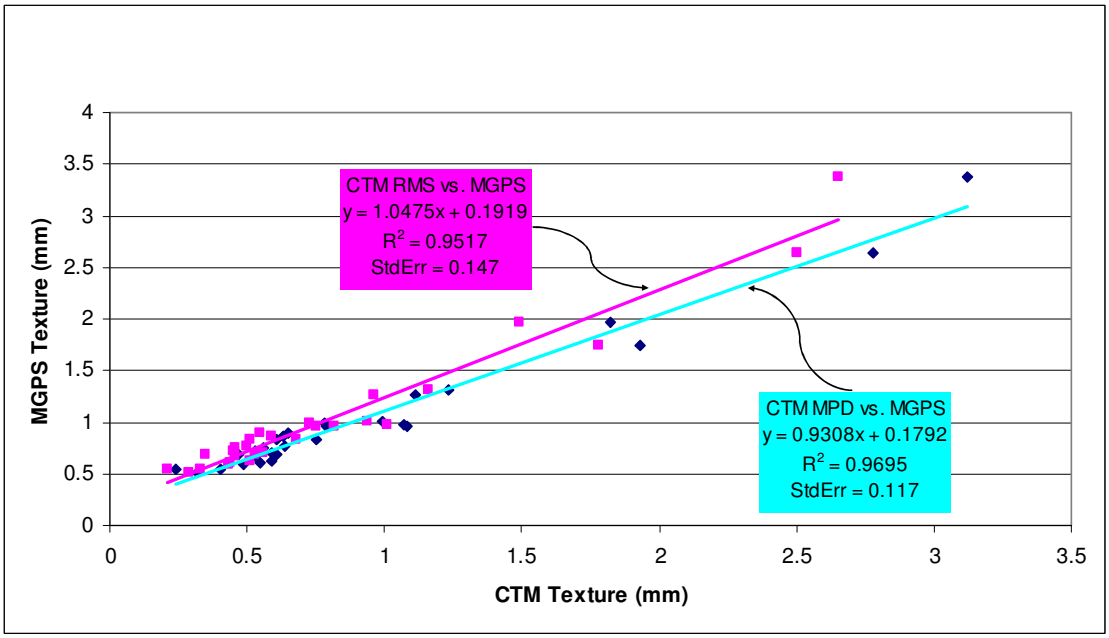

Figure C-10 Correlations between MGPS MPD and CTM Texture on Positive Texture

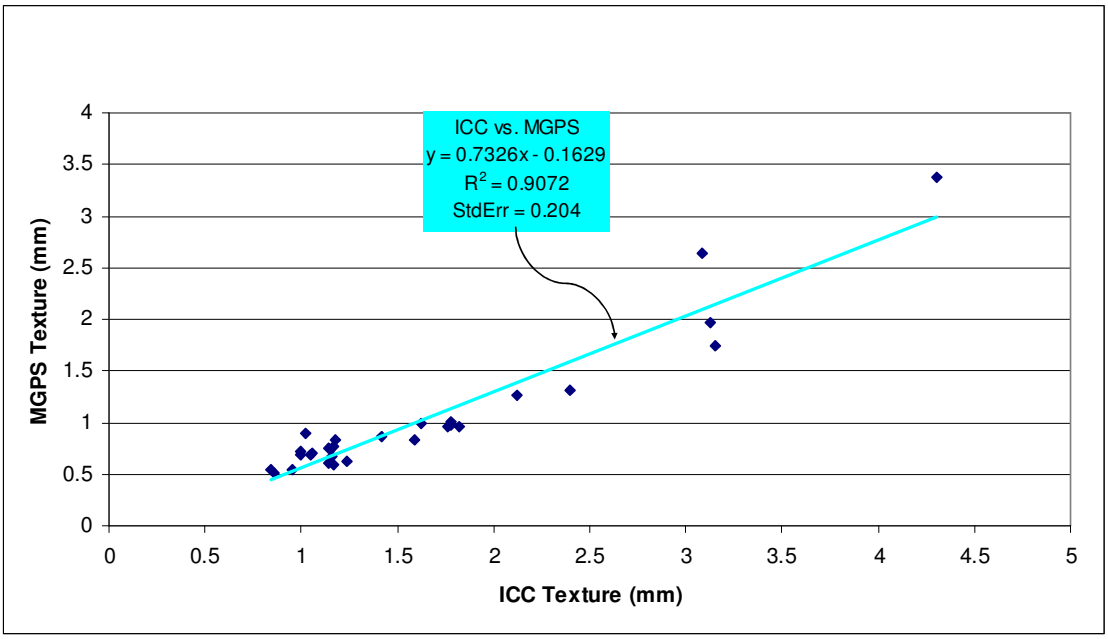

Figure C-11 Correlation between MGPS MPD and ICCTEX on Positive Texture

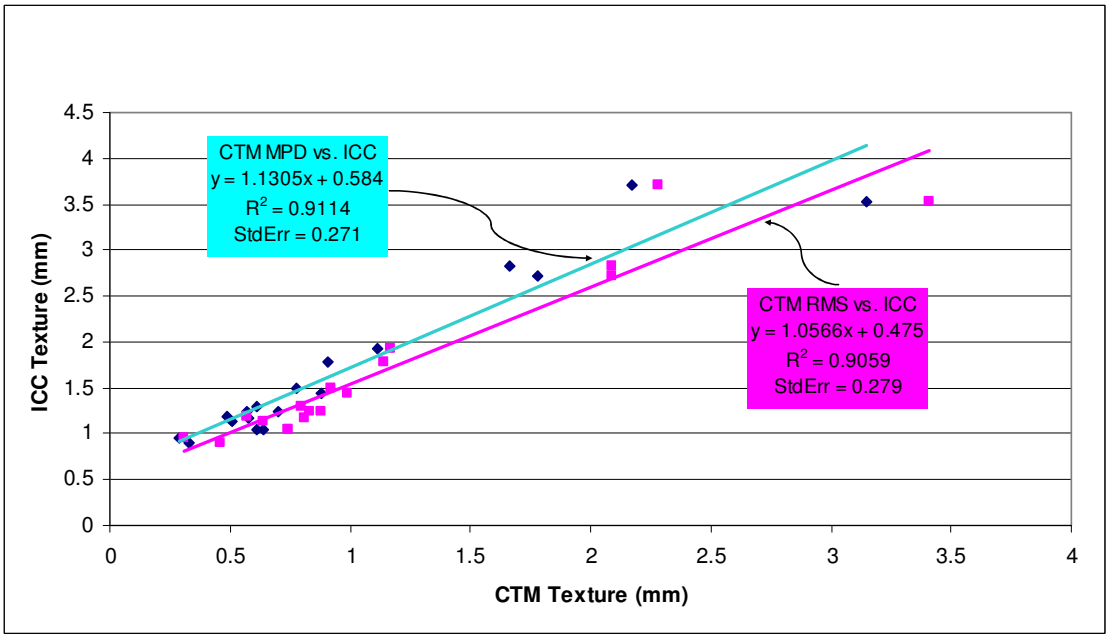

Figure C-12 Correlations between ICCTEX and CTM Texture on Negative Texture

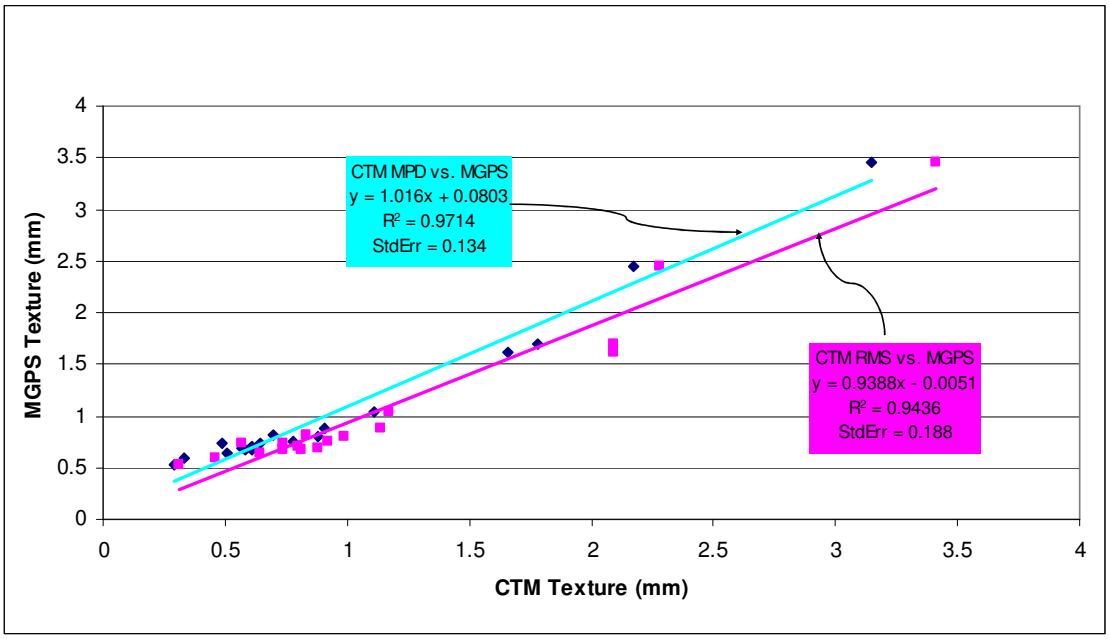

Figure C-13 Correlations between MGPS MPD and CTM Texture on Negative Texture

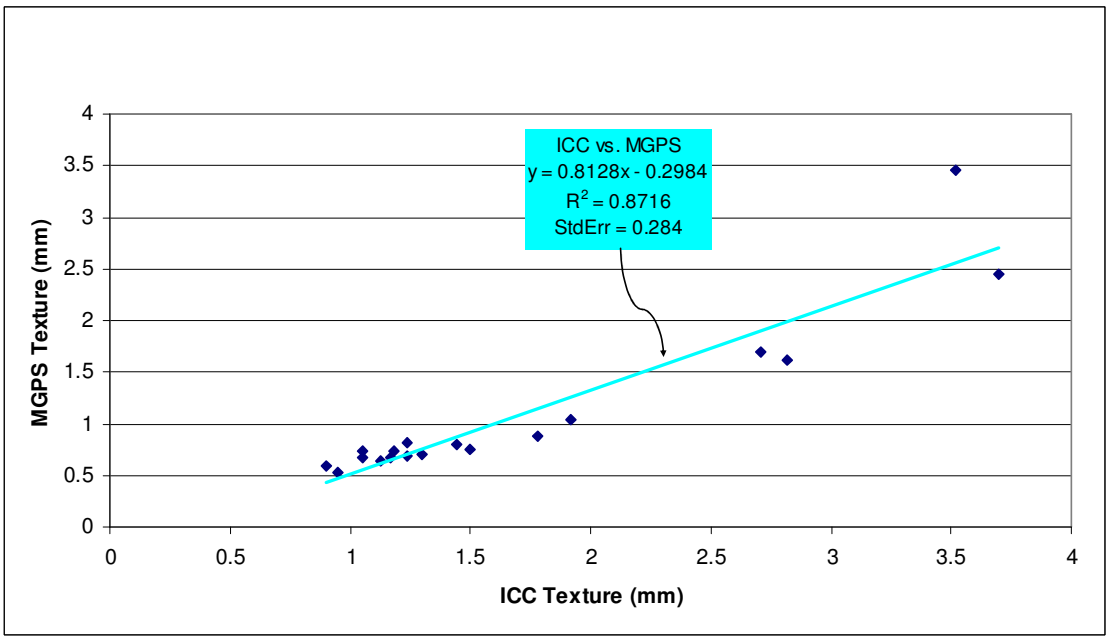

Figure C-14 Correlation between MGPS MPD and ICCTEX on Negative Texture

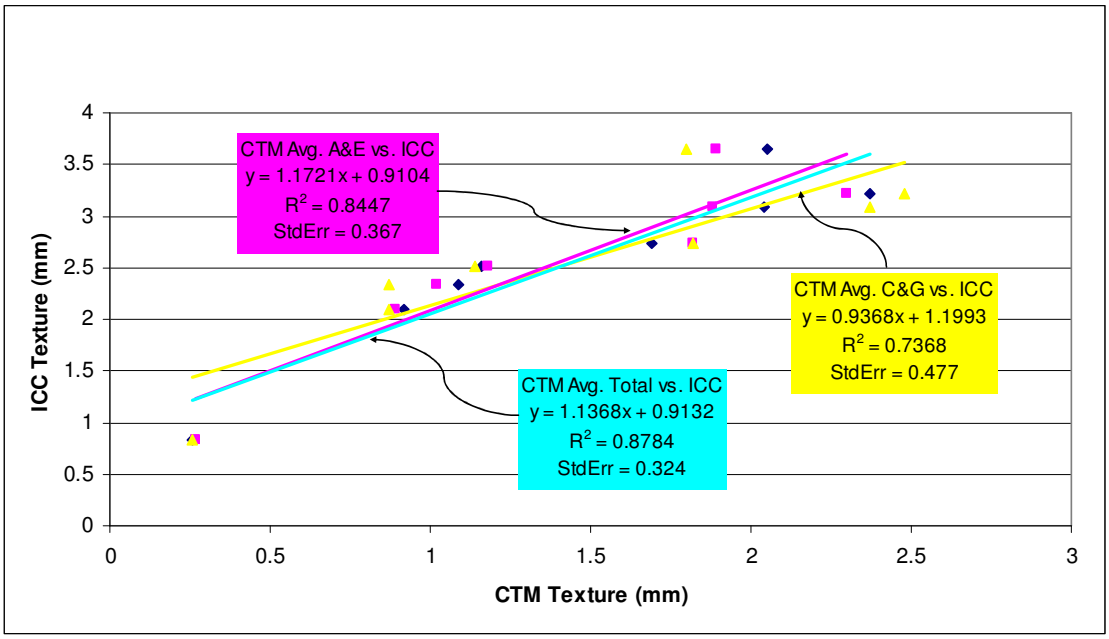

Figure C-15 Correlations between ICCTEX and CTM Texture on Neutral Texture

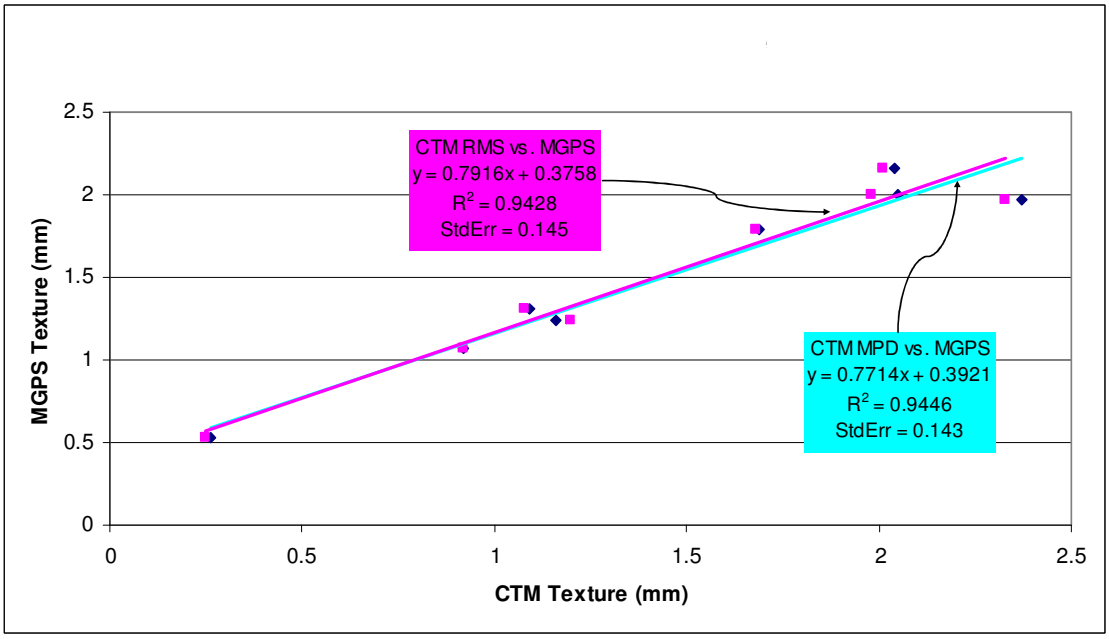

Figure C-16 Correlations between MGPS MPD and CTM Texture on Neutral Texture

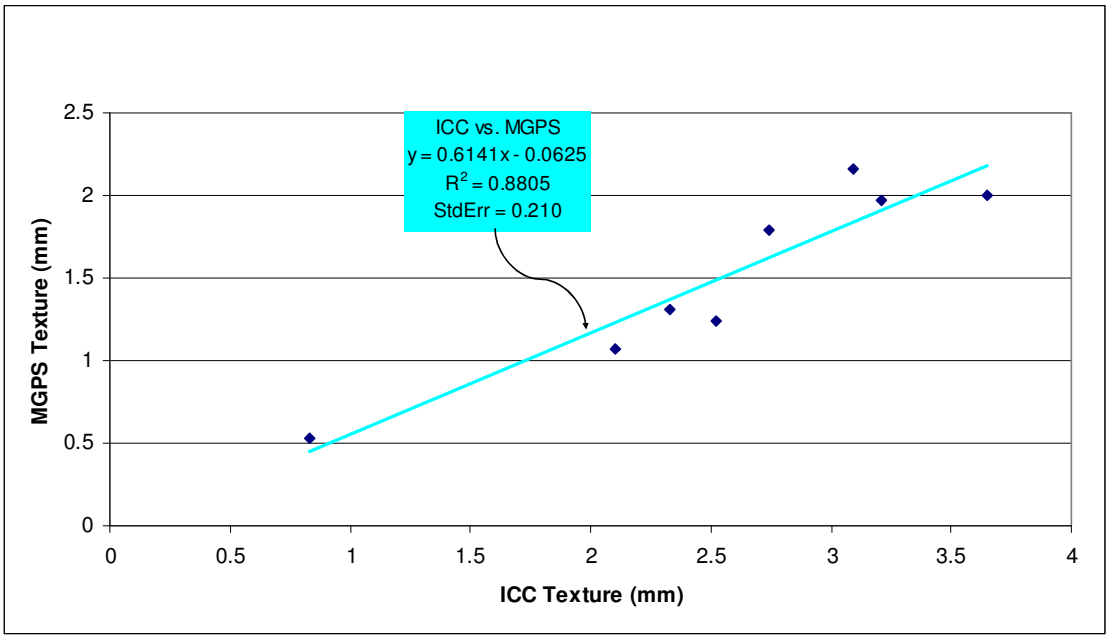

Figure C-17 Correlation between MGPS MPD and ICCTEX on Neutral Texture

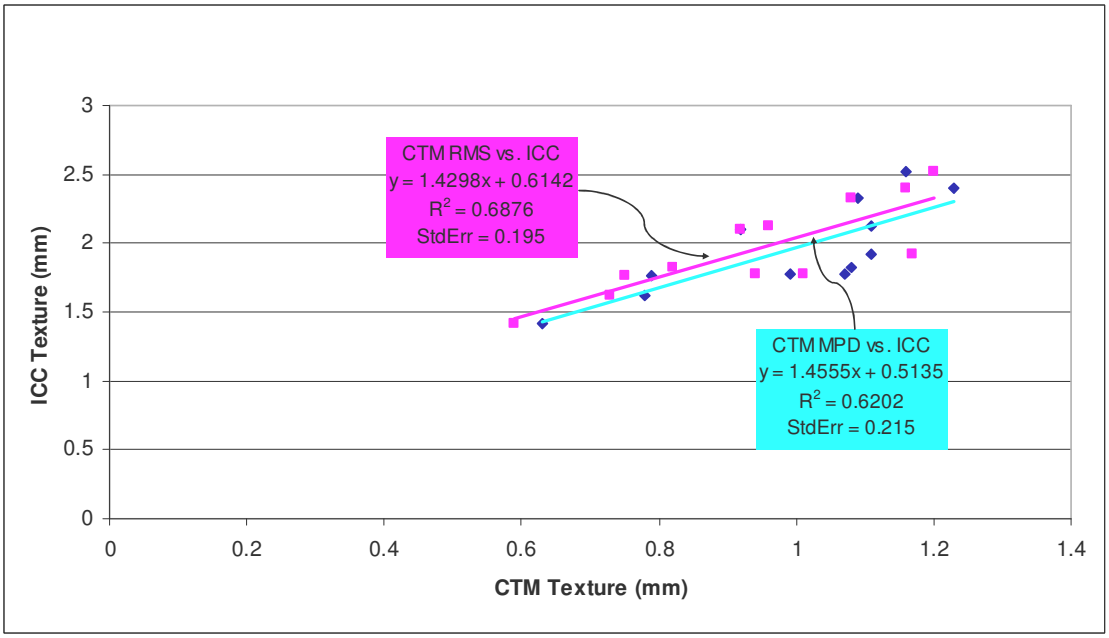

Figure C-18 Correlations between ICCTEX and CTM Texture on SMA Surfaces

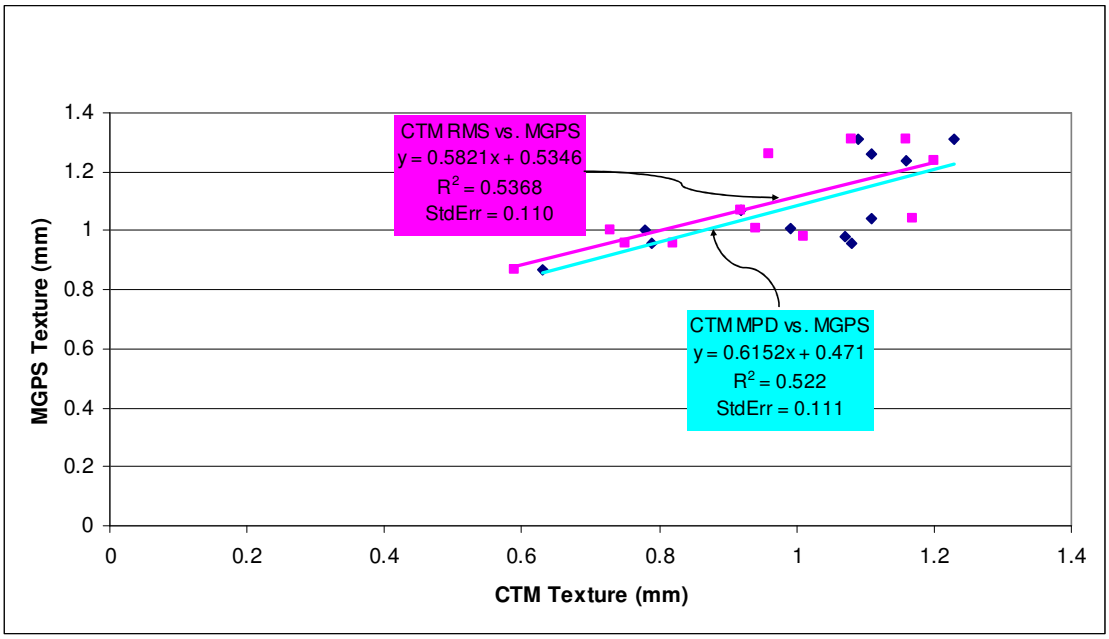

Figure C-19 Correlations between MGPS MPD and CTM Texture on SMA Surfaces

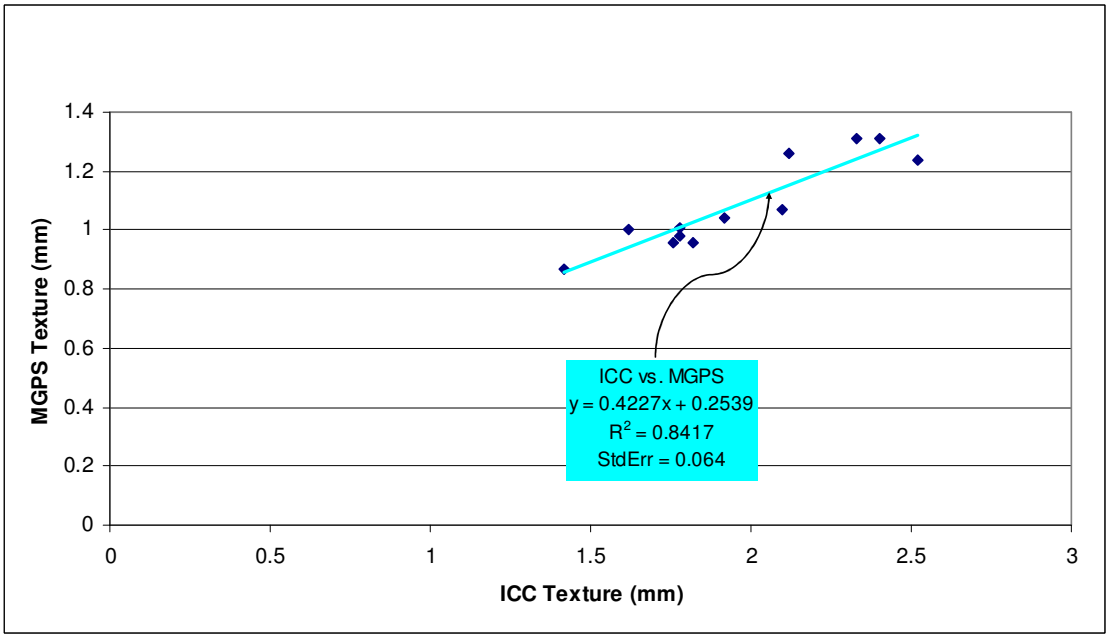

Figure C-20 Correlation between MGPS MPD and ICCTEX on SMA Surfaces

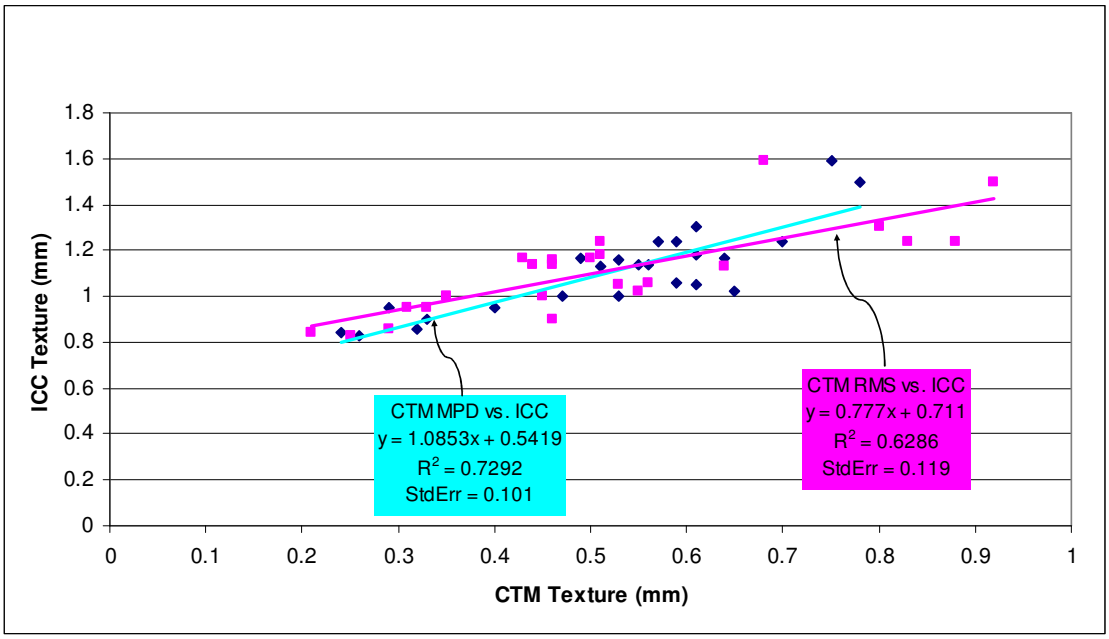

Figure C-21 Correlations between ICCTEX and CTM Texture on Dense-Asphalt Surfaces

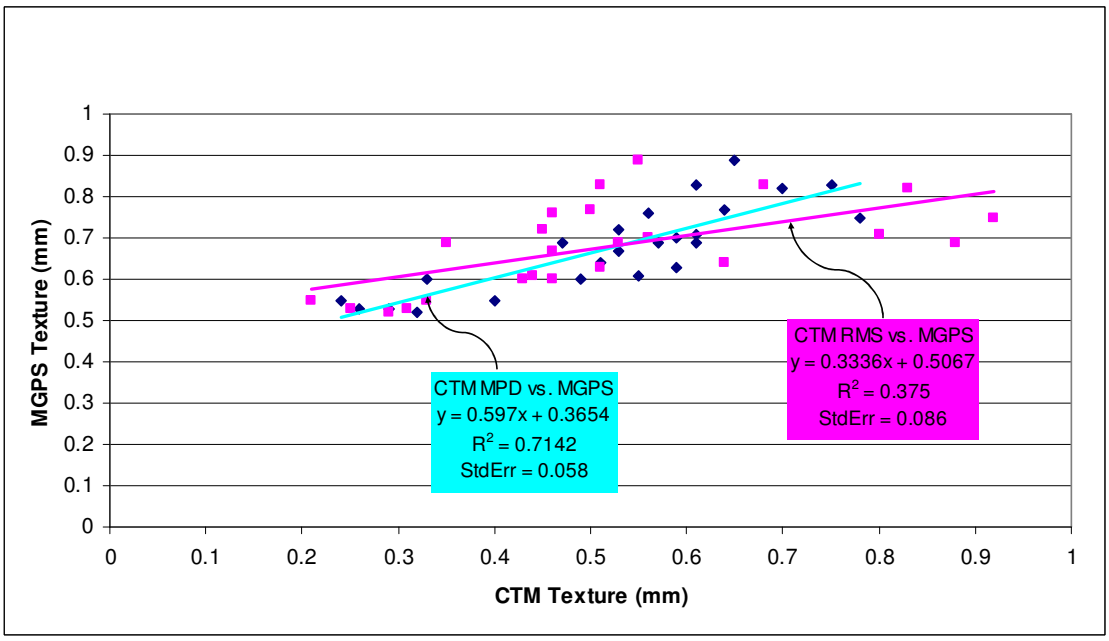

Figure C-22 Correlations between MGPS MPD and CTM Texture on Dense-Asphalt Surfaces

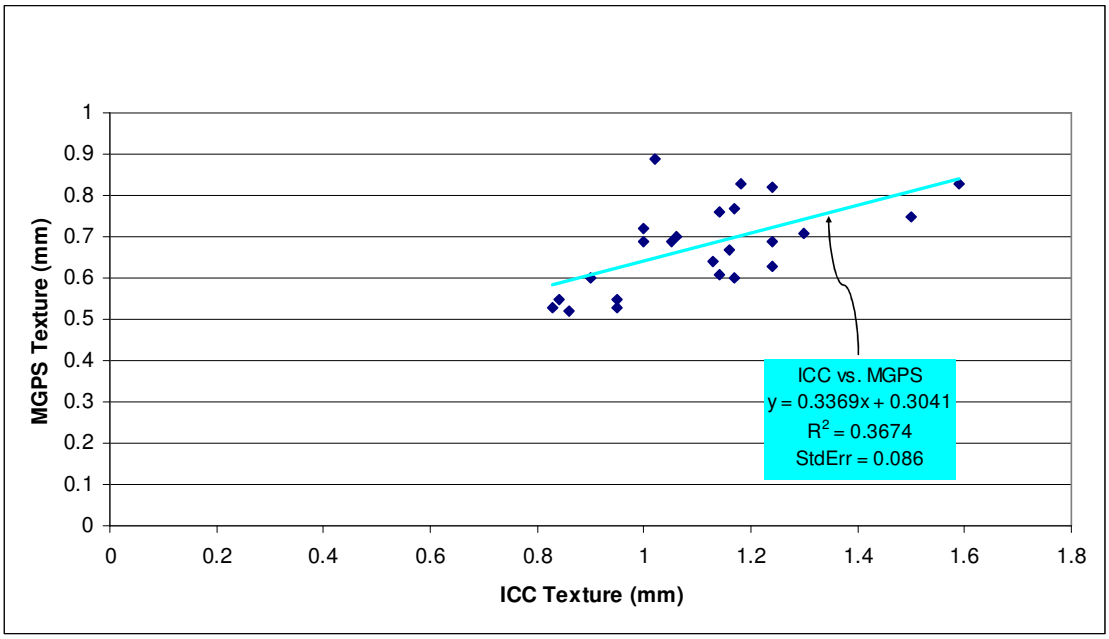

Figure C-23 Correlation between MGPS MPD and ICCTEX on Dense-Asphalt Surfaces

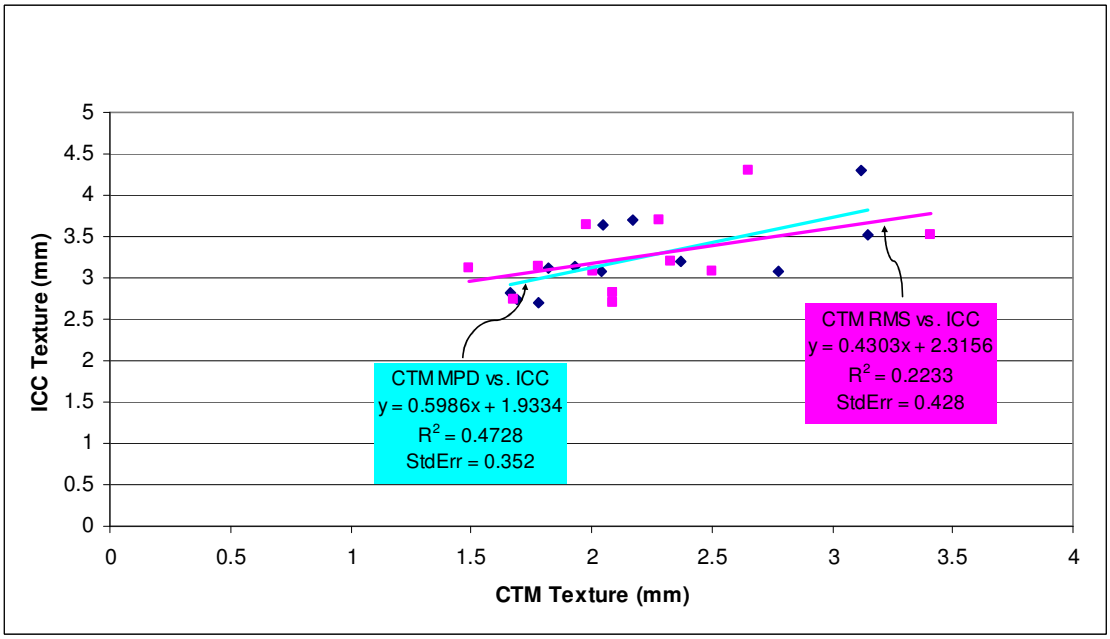

Figure C-24 Correlations between ICCTEX and CTM Texture on OGFC Surface

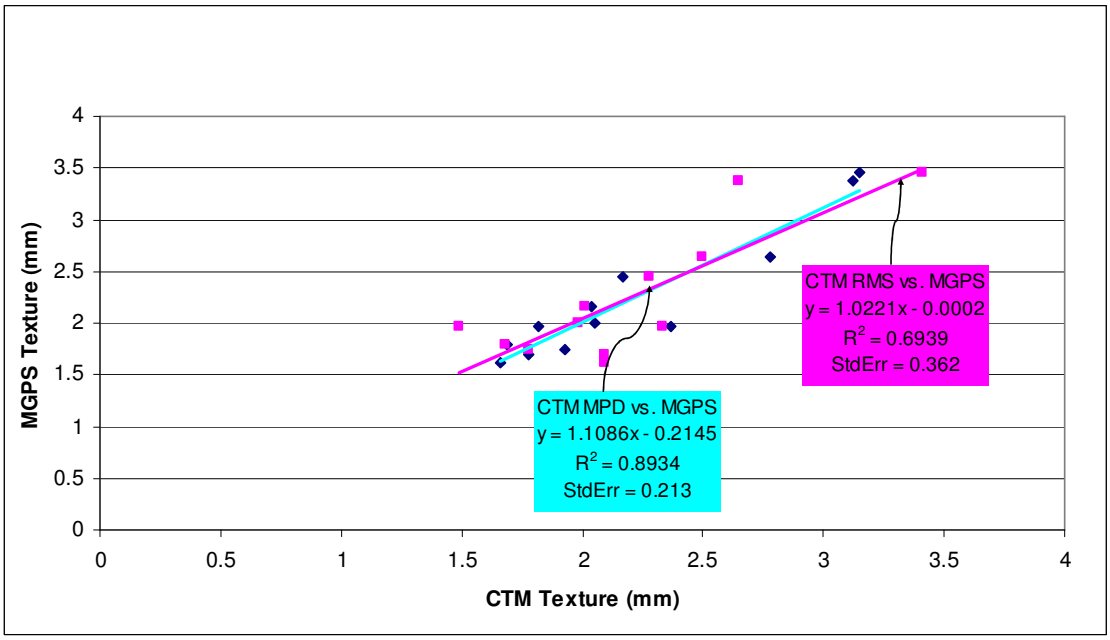

Figure C-25 Correlations between MGPS MPD and CTM Texture on OGFC Surface

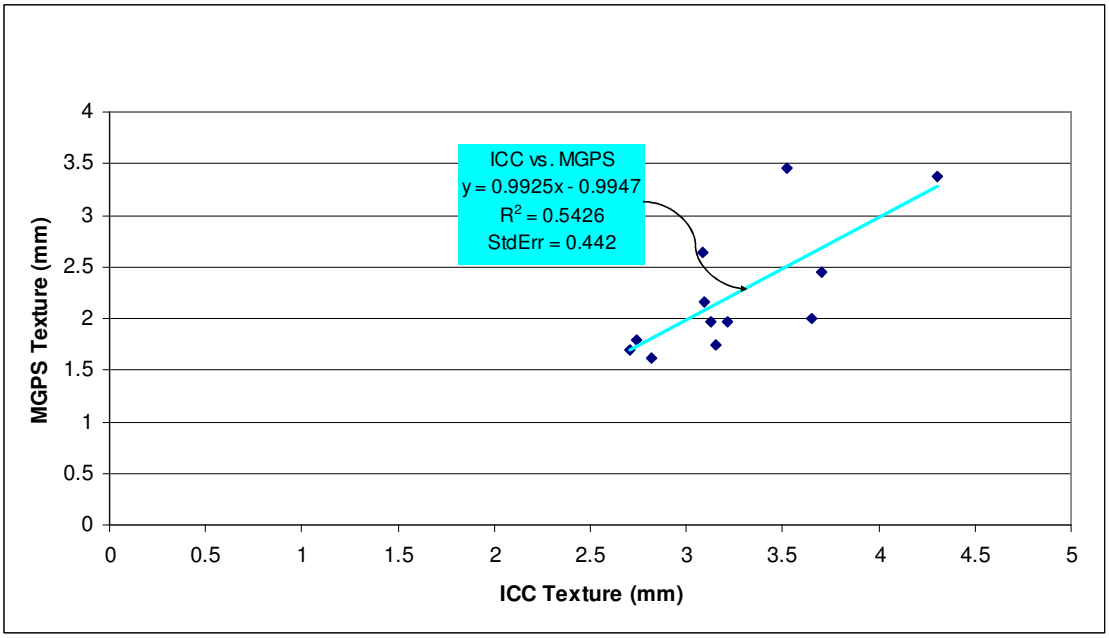

Figure C-26 Correlation between MGPS MPD and ICCTEX on OGFC Surface

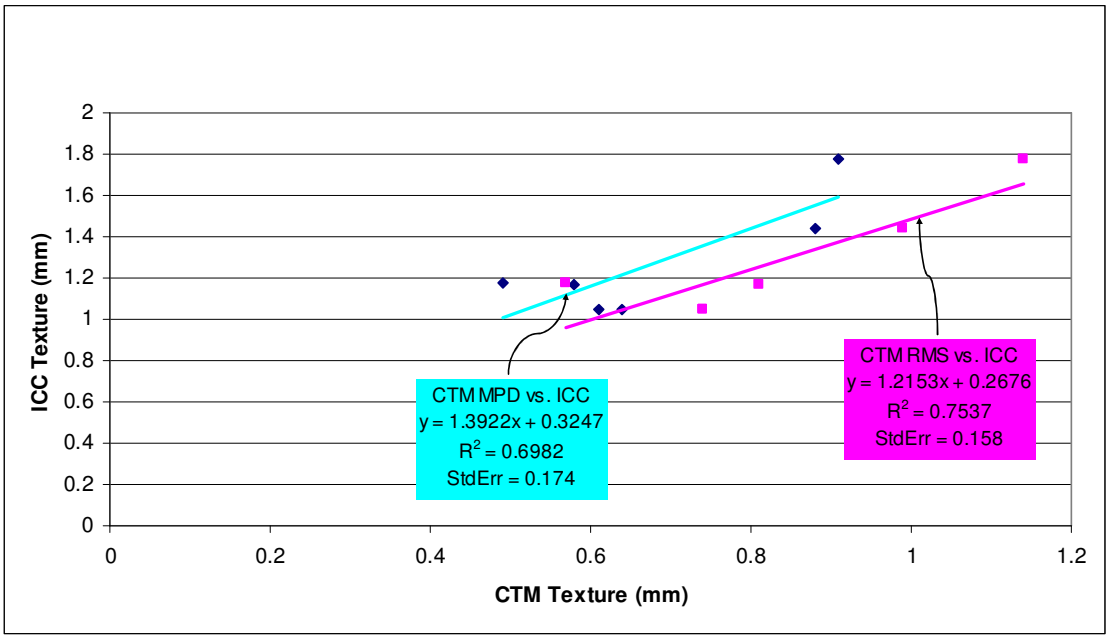

Figure C-27 Correlations between ICCTEX and CTM Texture on Concrete Surface

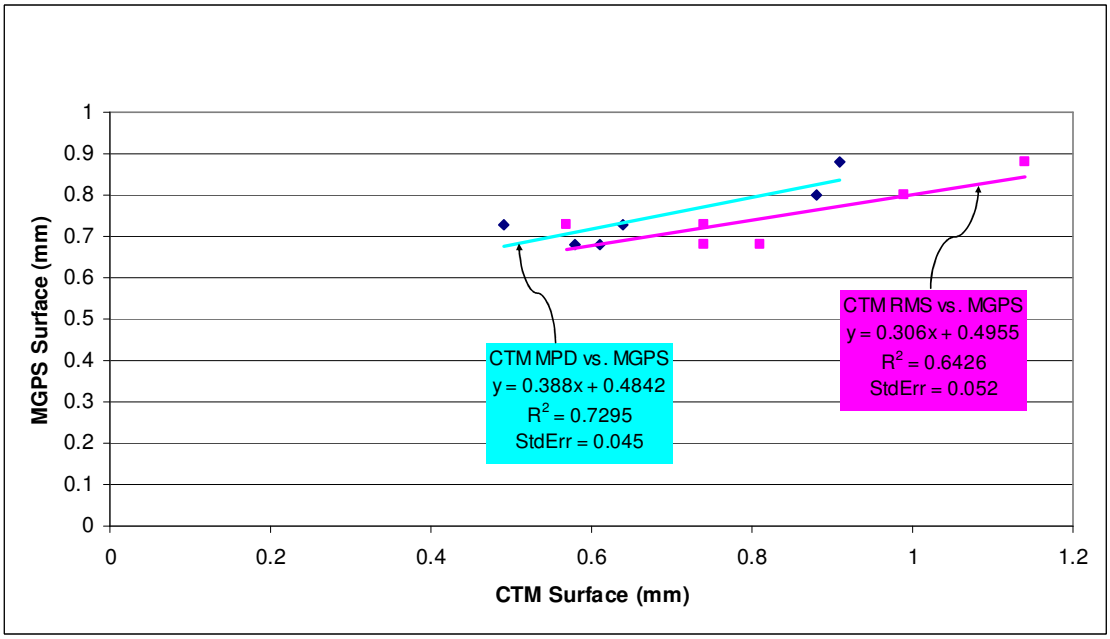

Figure C-28 Correlations between MGPS MPD and CTM Texture on Concrete Surface

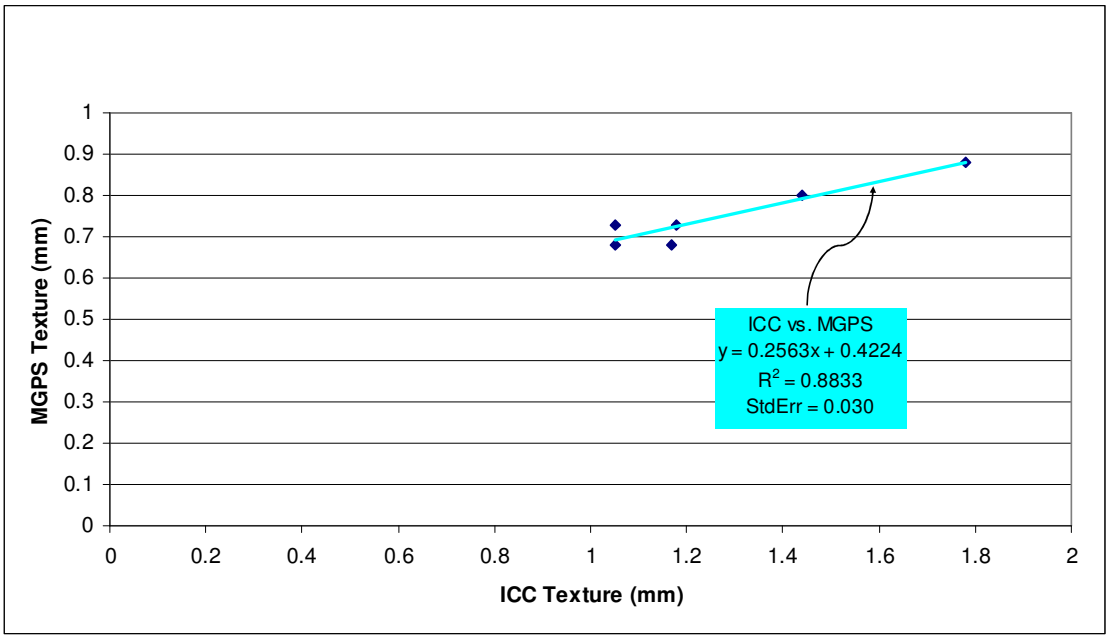

Figure C-29 Correlation between MGPS MPD and ICCTEX on Concrete Surface

APPENDIX D
MACROTEXTURE MEASUREMENTS AT THE VIRGINIA SMART ROAD ON AUGUST 17, 2001

Table D-1 Macrotexture measurements at the Virginia Smart Road on August 17, 2001 (Unit: mm)

Site	Location	CTM MPD	CTM_Long	CTM_Tran	CTM RMS	ICC Texture
Loop-EB	77.5', LWP	0.88	0.695	0.615	0.97	1.773
	77.5', BWP	1.17	1.16	1.25	1.28	2.13
	152.5', LWP	0.88	0.73	0.955	0.88	1.802
	152.5', BWP	1.13	1.125	1.205	1.18	2.25
	227.5', LWP	1.15	1.135	1.22	1.2	1.971
	227.5', BWP	1.28	0.98	1.435	1.44	2.039
C-EB	77.5', LWP	0.52	0.57	0.495	0.51	1.024
	77.5', BWP	0.59	0.7	0.57	0.62	1.24
	152.5', LWP	0.36	0.47	0.335	0.35	0.849
	152.5', BWP	0.38	0.33	0.445	0.4	0.952
	227.5', LWP	0.48	0.49	0.49	0.46	1.058
	227.5', BWP	0.6	0.49	0.82	0.64	1.098
D-EB	77.5', LWP	0.51	0.335	0.72	0.73	0.86
	77.5', BWP	0.54	0.515	0.485	0.65	1.064
	152.5', LWP	0.33	0.375	0.325	0.33	0.774
	152.5', BWP	0.61	0.495	0.71	0.61	1.228
	227.5', LWP	0.43	0.44	0.43	0.43	0.828
	227.5', BWP	0.71	0.725	0.735	0.73	1.224
G-EB	77.5', LWP	0.52	0.465	0.625	0.47	1.001
	77.5', BWP	0.5	0.46	0.49	0.48	1.108
	152.5', LWP	0.55	0.455	0.515	0.67	1.058
	152.5', BWP	0.62	0.59	0.665	0.53	1.093
	227.5', LWP	0.43	0.35	0.4	0.43	0.933
	227.5', BWP	0.6	0.66	0.43	0.56	1.083
J-EB	77.5', LWP	0.57	0.57	0.575	0.52	0.978
	77.5', BWP	0.48	0.405	0.505	0.42	1.042
	152.5', LWP	0.52	0.52	0.465	0.51	0.96
	152.5', BWP	0.53	0.56	0.585	0.49	1.237
	227.5', LWP	0.53	0.63	0.45	0.46	1.015
	227.5', BWP	0.56	0.695	0.43	0.47	1.122
K-EB	77.5', LWP	2.51	2.64	3.135	2.21	3.871
	77.5', BWP	2.66	3.035	2.425	3.32	4.241
	152.5', LWP	2.38	1.85	2.325	2.38	2.689
	152.5', BWP	2.31	2.25	2.79	2.02	3.287
	227.5', LWP	1.84	1.535	2.01	1.74	2.804
	227.5', BWP	1.8	1.53	1.77	1.46	3.11
L-EB	77.5', LWP	0.62	0.685	0.605	0.64	1.422
	77.5', BWP	1.17	1.04	1.255	1.11	1.821
	152.5', LWP	0.67	0.795	0.685	0.73	1.757
	152.5', BWP	1.22	1.115	1.345	1.38	1.958
	227.5', LWP	0.81	0.92	0.78	0.75	1.738
	227.5', BWP	1.43	1.76	1.355	1.45	2.15
K-WB	77.5', LWP	1.7	1.59	2.14	1.4	2.487
	77.5', BWP	2.4	2.765	1.905	2.19	3.656
	152.5', LWP	1.87	2.26	1.675	1.79	2.944
	152.5', BWP	2.47	2.43	2.75	2.26	3.78
	227.5', LWP	1.92	1.485	1.845	1.79	3.157
	227.5', BWP	2.34	2.195	2.62	2.18	3.758

APPENDIX E
MACROTEXTURE MEASUREMENTS AT THE NEWLY CONSTRUCTED HIGHWAY PROJECTS THROUGHOUT VIRGINIA

Table E-1 Macrotexture Measurements for Projects 02-1026, 02-1039, and 02-1041 (mm)

Project	Sample Location		CTM MPD	CTM-RMS	ICC
02-1026 I-81 SouthBound From Woodstock	LWP1	0	1.12	0.86	1.46
	LWP2	20	0.92	0.65	1.62
	LWP3	40	1.25	0.93	1.54
	LWP4	60	2.27	2.14	4.85
	LWP5	80	1.22	1.12	2.64
	LWP6	100	1.16	1.02	1.69
	LWP7	120	1.26	1.06	1.26
	BWP1	0	1.34	1.35	3.22
	BWP2	20	1.28	1.06	3.68
	BWP3	40	1.68	1.47	3.68
	BWP4	60	2.4	2.71	4.08
	BWP5	80	1.43	1.7	4.52
	BWP6	100	1.68	1.49	1.37
	BWP7	120	1.53	1.37	3.39
02-1039 Rt 7 West of Leesburg	LWP 1	0	0.53	0.43	1.04
	LWP 2	20	0.59	0.50	1.14
	LWP 3	40	0.60	0.46	1.43
	LWP 4	60	0.71	0.59	1.20
	LWP 5	80	0.63	0.59	1.29
	LWP 6	100	0.60	0.61	1.30
	LWP 7	120	0.60	0.53	1.21
	BWP 1	0	0.63	0.58	1.29
	BWP 2	20	0.55	0.51	1.62
	BWP 3	40	0.63	0.60	1.38
	BWP 4	60	0.64	0.57	1.51
	BWP 5	80	0.60	0.64	1.35
	BWP 6	100	0.64	0.66	1.50
	BWP 7	120	0.57	0.48	1.49
02-1041 Rt 7 East of Berrysville	LWP 1	0	1.01	1.18	1.78
	LWP 2	20	1.04	0.87	2.23
	LWP 3	40	1.05	0.77	1.73
	LWP 4	50	1.06	0.82	1.71
	LWP 5	55	0.76	0.67	1.61
	LWP 6	60	0.95	0.77	1.26
	LWP 7	65	1.08	0.82	1.58
	LWP 8	70	0.81	0.60	1.36
	LWP 9	80	0.91	0.78	1.64
	LWP 10	100	0.78	0.60	1.34
	LWP 11	120	0.70	0.59	1.69
	BWP 1	0	1.00	0.95	1.75
	BWP2	20	1.04	0.84	1.62
	BWP3	40	1.03	0.81	2.16
	BWP 4	50	0.99	0.81	1.94
	BWP 5	55	0.92	0.75	2.08
	BWP 6	60	1.22	1.56	1.93
	BWP 7	65	0.78	0.60	2.07
	BWP 8	70	0.84	0.69	1.47
	BWP 9	80	0.75	0.68	1.31
	BWP 10	100	0.67	0.55	1.44
	BWP 11	120	0.75	0.75	1.32

Table E-2 Macrotexture Measurements for Project 02-1043 and 02-1050 (mm)

Project	Sample Location		CTM MPD	CTM-RMS	ICC
02-1043 Rt. 15 East Gordansville	LWP 1	0	0.42	0.33	0.88
	LWP 2	20	0.44	0.35	0.82
	LWP 3	40	0.35	0.28	1.04
	LWP 4	50	0.46	0.37	1.07
	LWP 5	55	0.38	0.34	1.04
	LWP 6	60	0.57	0.44	0.86
	LWP 7	65	0.74	0.56	1.14
	LWP 8	70	0.57	0.42	1.33
	LWP 9	80	0.41	0.35	1.01
	LWP 10	100	0.34	0.26	1.18
	LWP 11	120	0.39	0.35	0.92
	BWP 1	0	0.43	0.34	0.95
	BWP2	20	0.35	0.29	0.89
	BWP3	40	0.54	0.56	0.97
	BWP 4	50	0.42	0.38	0.96
	BWP 5	55	0.40	0.52	0.88
	BWP 6	60	0.61	0.53	0.97
	BWP 7	65	0.75	0.55	1.15
	BWP 8	70	0.79	0.66	1.42
	BWP 9	80	0.73	0.67	1.12
	BWP 10	100	0.69	0.73	1.11
	BWP 11	120	0.74	0.91	1.02
02-1050 Rt. 522 West of Rt.3 in Culpeper	LWP 1	0	1.44	1.92	2.51
	LWP 2	20	1.36	1.40	2.55
	LWP 3	40	0.95	1.24	1.69
	LWP 4	50	1.12	1.18	2.06
	LWP 5	55	0.86	0.95	2.66
	LWP 6	60	1.16	1.31	1.96
	LWP 7	65	1.16	1.40	2.50
	LWP 8	70	1.18	1.29	2.03
	LWP 9	80	0.92	1.41	2.42
	LWP 10	100	0.92	0.89	1.78
	LWP 11	120	1.34	1.31	2.70
	BWP 1	0	0.84	1.12	1.99
	BWP2	20	0.68	0.68	1.52
	BWP3	40	0.71	0.69	1.81
	BWP 4	50	0.57	0.51	1.49
	BWP 5	55	0.63	0.60	2.26
	BWP 6	60	0.75	0.72	1.21
	BWP 7	65	0.98	1.05	1.57
	BWP 8	70	0.74	0.84	1.93
	BWP 9	80	0.86	0.80	1.62
	BWP 10	100	0.67	1.06	1.19
	BWP 11	120	0.55	0.65	1.07

Table E-3 Macrotexture Measurements for Project 02-1056 and 02-1068 (mm)

Project	Sample Location		CTM MPD	CTM-RMS	ICC
02-1056	LWP 1	0	0.71	0.90	2.85
Rt. 29 NB Danville	LWP 2	20	0.60	0.57	1.82
	LWP 3	40	0.61	0.68	1.55
	LWP 4	50	0.72	0.71	1.61
	LWP 5	55	0.62	0.68	1.54
	LWP 6	60	0.92	1.12	2.20
	LWP 7	65	0.95	0.89	1.98
	LWP 8	70	0.74	0.74	1.81
	LWP 9	80	0.73	0.75	1.76
	LWP 10	100	0.65	0.56	1.51
	LWP 11	120	0.63	0.72	1.62
	BWP 1	0	0.55	0.81	3.11
	BWP2	20	0.70	0.56	2.39
	BWP3	40	0.56	0.79	1.5
	BWP 4	50	0.55	0.60	1.57
	BWP 5	55	0.42	0.46	1.97
	BWP 6	60	0.43	0.56	1.8
	BWP 7	65	0.43	0.56	1.47
	BWP 8	70	0.48	0.51	1.42
	BWP 9	80	0.54	0.49	1.4
	BWP 10	100	0.58	0.64	1.9
	BWP 11	120	0.77	0.80	1.96
02-1068	LWP 1	0	0.53	0.48	1.70
Rt 33 West bound	LWP 2	20	0.65	0.59	1.18
From Elkton	LWP 3	40	0.88	0.77	1.45
	LWP 4	50	0.87	0.75	1.66
	LWP 5	55	1.30	1.17	2.03
	LWP 6	60	0.94	0.79	1.71
	LWP 7	65	1.07	1.23	2.15
	LWP 8	70	1.15	1.04	2.01
	LWP 9	80	0.74	0.67	1.75
	LWP 10	100	0.70	0.69	1.32
	LWP 11	120	0.84	0.69	1.52
	BWP 1	0	0.73	0.65	2.57
	BWP2	20	0.78	0.76	2.2
	BWP3	40	0.80	0.80	2.27
	BWP 4	50	1.35	1.14	3
	BWP 5	55	1.32	1.17	2.95
	BWP 6	60	1.19	1.08	2.36
	BWP 7	65	0.89	0.79	2.39
	BWP 8	70	0.79	0.75	2.22
	BWP 9	80	0.66	0.55	2.22
	BWP 10	100	0.57	0.55	2.14
	BWP 11	120	0.79	0.73	2.17

Table E-4 Macrotexture Measurements for Project 02-1079 (mm)

Project	Sample Location		CTM MPD	CTM-RMS	ICC
02-1079	LWP 1	0	0.75	0.81	1.75
Rt 460 East Bound	LWP 2	20	0.65	0.56	1.44
Tazewell	LWP 3	40	0.91	0.77	1.45
	LWP 4	50	1.14	1.03	2.64
	LWP 5	55	0.89	0.88	2.63
	LWP 6	60	1.75	1.85	3.17
	LWP 7	65	0.87	0.93	2.11
	LWP 8	70	1.14	1.08	2.33
	LWP 9	80	0.91	0.84	1.56
	LWP 10	100	0.82	0.82	1.56
	LWP 11	120	1.00	0.98	1.60
	BWP 1	0	0.75	0.69	1.52
	BWP2	20	0.54	0.73	1.29
	BWP3	40	0.67	0.64	1.35
	BWP 4	50	0.78	0.83	1.76
	BWP 5	55	0.62	0.62	2.14
	BWP 6	60	0.75	0.78	1.15
	BWP 7	65	0.73	0.68	1.64
	BWP 8	70	0.68	0.66	2.01
	BWP 9	80	0.72	0.79	1.32
	BWP 10	100	0.66	0.66	1.48
	BWP 11	120	0.63	0.77	1.2

APPENDIX F
MACROTEXTURE MEASUREMENTS AT THE WALLOPS FLIGHT FACILITY, VIRGINIA

Table F-1 Macrotexture Measurements at the Wallops Flight Facility (mm)

Site	1998 Data		1999 Data			
			First Data Set		Additional Texture-August	
	PSU MTD	CTM MPD	PSU MTD	CTM MPD	PSU MTD	CTM MPD
A	0.47	0.50	0.5	0.47	0.47	0.395
B	1.62	1.82	2.07	2.15	1.82	1.839
C	1.95	2.11	1.88	2.04	1.98	2.019
D	0.56	0.68	0.57	0.53	0.6	0.601
E	1.01	1.11	1.48	1.75	1.24	1.405
F	1.76	2.01	1.79	1.79	1.79	1.976
G	2.21	2.70				
K	0.48	0.65	0.46	0.49	0.46	0.541
K0	0.72	0.89	0.64	0.64	0.66	0.674
S0	0.50	0.48	0.7	0.57		
S1	0.73	0.65	0.6	0.64	0.66	0.614
S2	0.70	0.82	0.74	0.88	0.7	0.78
S3	1.03	1.19	1.19	1.29	1.06	1.07
S4	2.29	2.43	1.97	2.36	2.29	2.172
S5	1.31	1.29	1.06	1.02	1.19	1.186
S6	1.04	1.15	1.04	1.05		
MS1	0.47	0.57	1.18	1.16		
MS2	0.52	0.69	1.33	1.26		
MS3	0.50	0.62	1.27	1.12		
MS4	1.55	1.44				

VITAE

ManQuan Huang was born on November 30th 1979 in Dongguan City, Guangdong Province, the People's Republic of China. He graduated from DongGuan Middle School in July 1997. In July 2001, he received his Bachelor degree in Civil Engineering from the Tsinghua University in Beijing, China. Then he was sent to the Mechanic Institute of China Academic of Science for graduate study from September 2001 to May 2002 before he came to the United States. With the help of his kind advisors and friends, he earned his degree of Master of Science in May, 2004 from Virginia Tech. In June 2004, he will go back China to work for his country.